Autophagy 9:4, 510–527; April 2013; © 2013 Landes Bioscience

M98K-OPTN induces transferrin receptor degradation and RAB12-mediated autophagic death in retinal ganglion cells

Kapil Sirohi, Madhavi Latha Somaraju Chalasani, Cherukuri Sudhakar, Asha Kumari, Vegesna Radha* and Ghanshyam Swarup*

Centre for Cellular and Molecular Biology; Council of Scientific and Industrial Research; Hyderabad, India

Keywords: RAB12, autophagy, glaucoma, optineurin, retinal ganglion cells, transferrin receptor

Abbreviations: CASP, caspase; DAPI, 4',6-diamidino-2-phenylindole; EBSS, Earle's balanced salt solution; FAC, ferric ammonium citrate; LAMP1, lysosomal-associated membrane protein 1; LC3, microtubule-associated protein 1 light chain 3; LIR, LC3-interacting region; NAC, N-acetylcysteine; NTG, normal tension glaucoma; OPTN, optineurin; PARP1, poly (ADP-ribose) polymerase 1; POAG, primary open angle glaucoma; RGC, retinal ganglion cells; TF, transferrin; TFRC, transferrin receptor-1; TR-Dextran, Texas Red conjugated Dextran; shRNA, small-hairpin RNA; UBD, ubiquitin-binding domain; SOD2, superoxide dismutase 2, mitochondrial; WT, wild type

Mutations in the autophagy receptor OPTN/optineurin are associated with the pathogenesis of glaucoma and amyotrophic lateral sclerosis, but the underlying molecular basis is poorly understood. The OPTN variant, M98K has been described as a risk factor for normal tension glaucoma in some ethnic groups. Here, we examined the consequence of the M98K mutation in affecting cellular functions of OPTN. Overexpression of M98K-OPTN induced death of retinal ganglion cells (RGC-5 cell line), but not of other neuronal and non-neuronal cells. Enhanced levels of the autophagy marker, LC3-II, a post-translationally modified form of LC3, in M98K-OPTN-expressing cells and the inability of an LC3-binding-defective M98K variant of OPTN to induce cell death, suggested that autophagy contributes to cell death. Knockdown of *Atg5* reduced M98K-induced death of RGC-5 cells, further supporting the involvement of autophagy. Overexpression of M98K-OPTN enhanced autophagosome formation and potentiated the delivery of transferrin receptor to autophagosomes for degradation resulting in reduced cellular transferrin receptor levels. Coexpression of transferrin receptor or supplementation of media with an iron donor reduced M98K-induced cell death. OPTN complexes with RAB12, a GTPase involved in vesicle trafficking, and M98K variant shows enhanced colocalization with RAB12. Knockdown of *Rab12* increased transferrin receptor level and reduced M98K-induced cell death. RAB12 is present in autophagosomes and knockdown of *Rab12* resulted in reduced formation of autolysosomes during starvation-induced autophagy, implicating a role for RAB12 in autophagy. These results also show that transferrin receptor degradation and autophagy play a crucial role in RGC-5 cell death induced by M98K variant of OPTN.

Introduction

OPTN is a ubiquitously expressed protein, and mutations in the coding region of the *OPTN* gene are associated with glaucoma and amyotrophic lateral sclerosis.[1,2] Glaucoma is a complex and genetically heterogeneous neurodegenerative eye disease with progressive loss of retinal ganglion cells (RGCs) in the optic disc and understanding its etiopathogenesis is important for its management.[3] Association of OPTN mutations and polymorphisms with glaucoma varies among geographically distinct populations.[4,5] Many mutations such as the E50K, T202R, E322K, H486R, H26D and M98K variant have been reported in OPTN which are mainly associated with normal tension glaucoma (NTG), a subtype of adult onset primary open angle glaucoma (POAG).[1,5-8] E50K mutation is the most severe disease-causing mutation of OPTN that is associated with 16.7% cases of familial NTG.[1] The same study showed that amino acid change in OPTN at the 98th position from Met to Lys (M98K) was found in 13.6% of NTG subjects compared with 2.1% in control individuals. Several reports that followed have shown M98K polymorphism in OPTN to be associated with glaucoma in Japanese, Chinese and Indian populations but not in Caucasian populations.[4,6,8-10] A study from southern India has shown that the M98K variant is associated with 6% of NTG and 4% POAG cases while there was no M98K variant found in control cases.[10]

OPTN protein consists of 577 amino acids organized into various domains such as a zinc-finger domain, ubiquitin-binding domain (UBD), leucine-zipper domain and LC3-interacting

*Correspondence to: Vegesna Radha and Ghanshyam Swarup; Email: vradha@ccmb.res.in and gshyam@ccmb.res.in
Submitted: 06/27/12; Revised: 12/25/12; Accepted: 01/02/13
http://dx.doi.org/10.4161/auto.23458

region (LIR) through which it is known to interact with a large number of proteins.[11-16] OPTN homo-oligomerizes when overexpressed and it forms juxta-nuclear foci.[16] Its expression is high in the retina, heart, brain and kidney.[17] Glaucoma-associated mutations in OPTN have been found in almost all parts of the molecule and are not clustered in any specific region.[5-10] By functioning as an adaptor for interaction with a variety of molecules, OPTN plays a role in cellular functions such as vesicular trafficking, cytoskeletal organization, signal transduction and autophagy.[13-15,18-25] Deregulated cellular OPTN levels or mutant protein may disturb cellular homeostasis due to altered interactions and multimolecular complex formation. Endogenous OPTN primarily localizes to the cytoplasm and shows prominence in the Golgi region.[1,19,26] It is involved in Golgi organization and exocytosis through regulation of secretory vesicle fusion in the plasma membrane.[19,27] Presently, we lack an understanding of how mutations in OPTN alter its normal function to cause pathology. It has been shown earlier that the E50K mutation impairs endocytic recycling of transferrin receptor (TFRC) and causes death of RGCs.[15,28,29] E50K-overexpressing transgenic mice showed massive apoptosis, increased autophagy in RGCs and degeneration of the retina.[30,31] This mutation has been shown to alter the interaction between OPTN and RAB8A, a GTPase involved in regulation of vesicular trafficking.[15,30,32] The E50K-induced inhibition of endocytic recycling of TFRC is due to inactivation of RAB8A that is mediated by TBC1D17, a GTPase activating protein.[32] OPTN interacts with ubiquitinated TFRC through its UBD and knockdown of cellular OPTN impairs TFRC trafficking to the juxta-nuclear regions.[15] Altered interactions of E50K mutant with TFRC and RAB8A possibly contribute to impaired recycling of TFRC which may be responsible for this mutant triggering cell death signaling. However, functional defects caused by M98K variant of OPTN are not known.

Autophagy is a quality control mechanism to remove defective proteins and organelles. It is defined as a process by which cytoplasmic components including organelles reach the lysosomes for degradation. It is essential for homeostasis of neuronal cells and its dysregulation is involved in several neurodegenerative disorders.[33] Recently, OPTN has been identified as an autophagy receptor that is involved in clearance of cytosolic *Salmonella*.[14] Autophagy receptors play an essential role in cargo selection by simultaneously binding cargo as well as LC3 present on autophagosomal membranes and deliver the cargo to autophagosomes. OPTN binds to LC3 and ubiquitin, and these interactions are required for clearance of ubiquitinated bacteria.[14] However, no specific protein ligand which is targeted for autophagic degradation has been identified for OPTN. Overexpression of wild-type (WT) OPTN and its mutant E50K results in the formation of autophagosomes.[31]

Endocytosis of iron-bound transferrin by the TFRC plays an important role in regulating cellular iron homeostasis. Upon release of iron, the internalized receptor is recycled back to the cell membrane through early endosomes or recycling endosomes.[34] Recently, it has been shown that TFRC is constitutively processed through the lysosomal compartment, mediated by RAB12, a GTPase involved in vesicle trafficking.[35] In the presence of excess iron, ubiquitination of cellular TFRC is enhanced, leading to its increased degradation in lysosomes independent of RAB12.[36,37] In this study, we aimed at understanding how the glaucoma-associated M98K variant alters cellular functions thereby causing pathology. Using RGC-5 cell line as a model for retinal ganglion cells,[38,39] we showed that M98K variant of OPTN induces cell death selectively in RGC-5 cells. Overexpressed M98K causes degradation of cellular TFRC protein through the autophagosomal-lysosomal pathway. We have investigated the role of TFRC degradation and RAB12 in M98K-induced death of RGC-5 cells that involves autophagy.

Results

Expression of M98K variant of OPTN induces death selectively in RGC-5 cells. Patients with POAG/NTG have shown higher incidence of E50K, E322K, M98K, and T202R mutations in OPTN compared with control subjects.[1,4,6,7,9] These point mutations localize to various domains of OPTN (**Fig. 1A**). Earlier findings showed that the E50K mutant of OPTN caused death in RGC-5 cells, mediated by oxidative stress.[28] In order to observe the effects of overexpression of other glaucoma-associated mutants of OPTN in retinal ganglion cells, RGC-5 cells grown on coverslips were transiently transfected with HA-tagged OPTN and its mutants and stained using anti-HA antibody and DAPI. Cells were observed using a fluorescence microscope to detect morphological features of cell death in expressing and non-expressing cells (**Fig. 1B**). Upon expression of the M98K variant, several cells showed loss of refractility, chromatin condensation, cytoplasmic shrinkage and membrane blebbing which are hallmarks of apoptosis. Overexpression of M98K caused death in 12.83 ± 3.12% of expressing cells, while E322K and T202R mutants did not show higher cell death compared with WT-OPTN (**Fig. 1C**). Cell death induced by M98K was not due to difference in expression levels compared with WT-OPTN or other mutants used (**Fig. 1D**). Untagged and GFP-tagged M98K variant expression also resulted in higher cell death compared with the corresponding WT counterparts (data not shown). Expression of M98K-OPTN did not cause death in other cell lines like IMR-32, HeLa and Cos-1 when quantitated at 32 h after transfection (**Fig. 1E**).

To characterize the mechanism of cell death induced by M98K, and determine which caspases were engaged, dominant negative mutants of caspase 9 (CASP9) and caspase 1 (CASP1) were coexpressed with M98K. Cell death caused by M98K was significantly reduced by both these mutant caspases indicating that M98K-induced cell death was dependent on the function of CASP1 as well as CASP9 (**Fig. S1A**, upper panel). Expression of these caspases did not significantly affect expression of M98K (**Fig. S1A**, lower panel). CASP3 is an executioner caspase, involved in intrinsic as well as extrinsic apoptotic pathways. M98K expression in RGC-5 cells resulted in CASP3 activation as detected by cleaved CASP3 and cleaved PARP1 bands in western blots (**Fig. 1F**). No activation of CASP3 was observed in other cell lines upon M98K overexpression (**Fig. 1G**). These

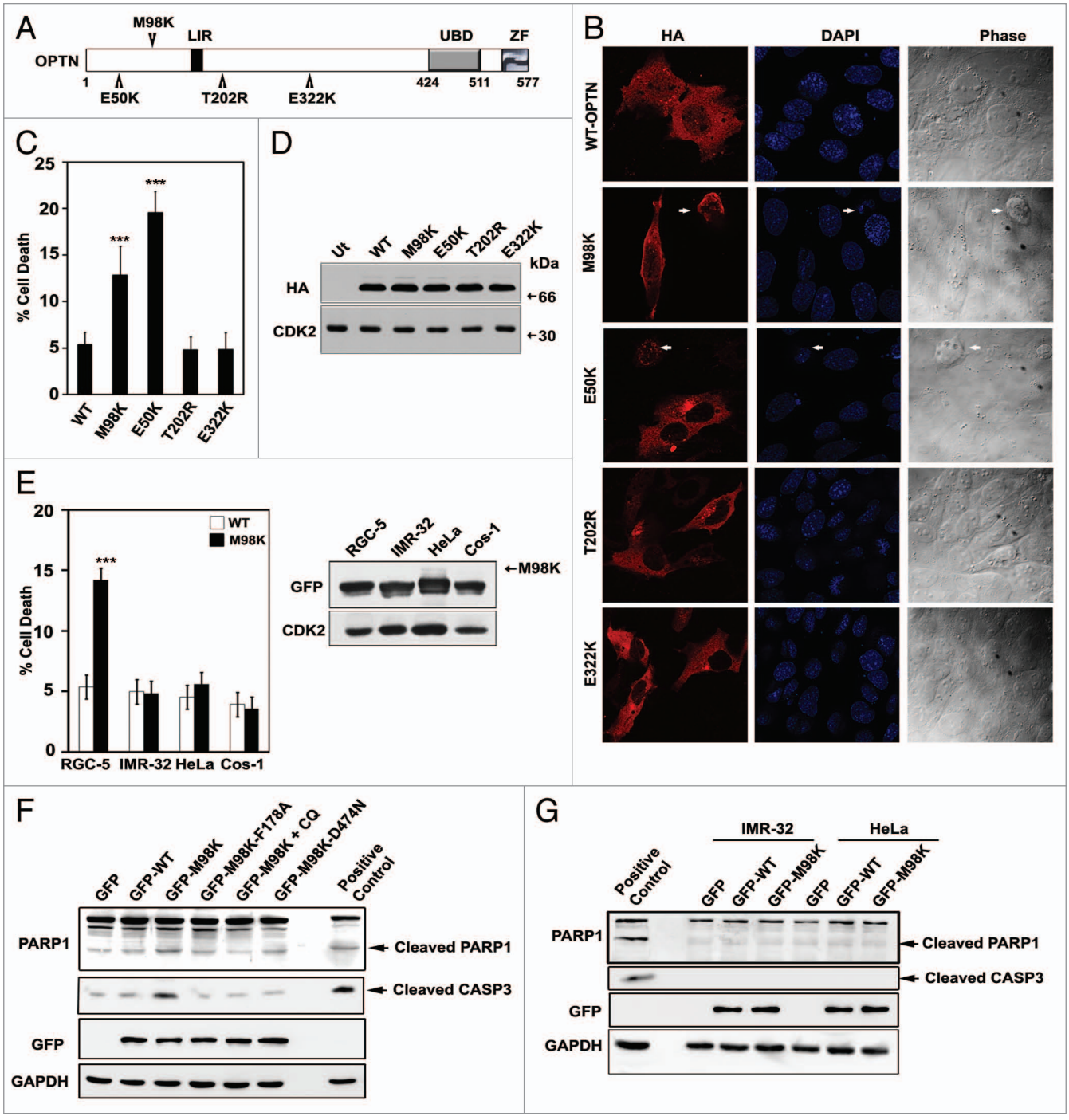

Figure 1. Expression of M98K variant of OPTN induces cell death selectively in RGC-5 cells. (**A**) Schematic of OPTN showing various domains and position of different mutations. LIR, LC3-interacting region; UBD, ubiquitin-binding domain; ZF, zinc-finger domain. (**B**) RGC-5 cells were transfected with HA-tagged constructs of WT-OPTN or various mutants as indicated and stained with HA antibody to detect expressing cells. Panels show images captured using 63× objective of Axioplan2 microscope (Zeiss). DAPI and phase panels indicate nuclear and cell morphology. Arrows indicate apoptotic cells. (**C**) Quantitation of cell death induced by WT-OPTN and its mutants in RGC-5 cells upon 32 h of expression. Data represent mean ± s.d of percentage of expressing cells showing apoptotic morphology after subtraction of cell death seen in non-expressing cells, from at least three independent experiments using duplicate coverslips. n = 6, ***$p < 0.001$. (**D**) Western blot showing expression levels of various constructs of OPTN under conditions used for apoptotic assays. CDK2 was used as loading control. Ut, untransfected. (**E**) Left panel, quantitation of cell death induced by WT-OPTN and M98K in various cell lines. Data are represented as in (**C**). n = 6, ***$p < 0.001$. Right panel, levels of overexpressed M98K in whole cell lysates of indicated cell lines is shown in the western blot. (**F**) M98K expression causes cleavage of CASP3 and PARP1. Western blots showing cleavage of CASP3 and PARP1 upon overexpression of WT-OPTN, M98K-OPTN (in the presence and absence of chloroquine) and other mutants of M98K in RGC-5 cells. GAPDH was used as loading control. Positive control, RGC-5 cells treated with 10 ng/ml TNF and 20 μg/ml cycloheximide for 8 h; CQ, chloroquine. (**G**) Western blots showing cleavage of CASP3 and PARP1 upon overexpression of WT-OPTN and M98K in IMR-32 and HeLa cells.

results suggested that M98K induced caspase-mediated cell death in RGC-5 cells.

Overexpression of BCL2 is generally known to inhibit cell death mediated through the release of mitochondrial components and E50K-induced cell death was inhibited by BCL2 coexpression.[28] In contrast, we found that M98K-induced cell death was not inhibited by BCL2 overexpression (**Fig. S1B**). E50K-mediated cell death was earlier shown to be rescued by antioxidants.[28] Treatment of M98K transfected cells with an antioxidant, N-acetylcysteine (NAC), or cotransfection with a plasmid expressing superoxide dismutase 2, mitochondrial (SOD2), a mitochondrial enzyme, did not significantly reduce cell death, suggesting that oxidative stress is not a key player in cell death induced by M98K (**Fig. S1C**).

M98K-OPTN shows enhanced interaction and colocalization with TFRC and inhibits uptake of transferrin. Upon overexpression, M98K-OPTN formed larger and more foci compared with the WT-OPTN (**Fig. 2A**). We have previously reported that OPTN interacts and colocalizes with TFRC.[15] TFRC facilitates the uptake of extracellular iron bound to transferrin by endocytosis after which it is recycled to the plasma membrane. We examined whether M98K differs in interaction with endogenous TFRC compared with WT-OPTN. RGC-5 cells were infected with adenoviruses expressing HA-tagged WT or M98K-OPTN for 18 h and lysates were subjected to immunoprecipitation using HA antibody. Upon western blotting, M98K immunoprecipitate showed higher levels of TFRC compared with WT-OPTN immunoprecipitate (**Fig. 2B**) suggesting that M98K variant shows stronger interaction with TFRC. To determine if M98K also showed better colocalization with TFRC, RGC-5 cells were transfected with either GFP-M98K or GFP-WT OPTN for 24 h. Immunostaining for endogenous TFRC showed strong colocalization of TFRC with M98K in vesicle-like structures formed by M98K (**Fig. 2C**). WT-OPTN showed lower correlation coefficient of colocalization with TFRC as compared with M98K (**Fig. 2D**).

Since M98K showed stronger colocalization and interaction with TFRC compared with WT-OPTN, one of the direct effects of this could be impaired trafficking of TFRC. To examine this, RGC-5 cells transfected with WT or M98K-OPTN were incubated with Alexa-546-conjugated transferrin (TF-Alexa-546) for 15 min. Quantitative analysis showed 43% inhibition in transferrin uptake in cells expressing M98K compared with nonexpressing cells while WT-expressing cells showed no significant inhibition (**Fig. 2E and F**). We also observed less colocalization between TF-Alexa-546 and TFRC in M98K-expressing cells, whereas, the nonexpressing cells showed good colocalization (**Fig. 2G**).

The E50K mutant of OPTN inhibits transferrin uptake and TF/TFRC recycling.[15,29] This inhibitory effect of E50K is due to inactivation of RAB8A that is mediated by TBC1D17, a GTPase-activating protein.[32] The E50K mutant shows loss of direct interaction with RAB8A (as seen by yeast two-hybrid assay),[32] but enhanced indirect interaction (as seen by immunoprecipitation).[15] The M98K mutant did not show any difference in interaction with RAB8A or activated RAB8A (Q67L-RAB8A) in a yeast two-hybrid assay (**Fig. S2A**) but it showed increased colocalization with RAB8A (**Fig. S2B**). These results indicated that M98K differs in engagement of downstream effectors regulating TFRC homeostasis compared with E50K.

M98K-OPTN reduces TFRC level through lysosomal degradation. The reduction in transferrin uptake could be because of reduced levels of TFRC, slow trafficking or recycling of TFRC to the plasma membrane in M98K-expressing cells. We observed that adenovirus mediated overexpression of M98K caused reduction in cellular TFRC levels (**Fig. 3A**). Expression of E50K mutant or WT-OPTN did not reduce TFRC levels (**Fig. 3A**). Reduction in TFRC levels upon M98K overexpression was not seen in IMR-32 and HeLa cells (**Fig. 3B**).

Proteasomal and lysosomal pathways are the two major mechanisms for degradation of cellular proteins. Inhibition of proteasomal pathway by MG-132 (5 μM) for 12 h did not restore the TFRC levels in RGC-5 cells expressing M98K (**Fig. 3C**). Treatment with lysosomal inhibitors, chloroquine (25 and 50 μM) and ammonium chloride (10 and 20 mM), for 18 h prevented reduction of TFRC levels observed in M98K-expressing cells (**Fig. 3D**). These results suggested that overexpression of M98K induced the degradation of TFRC through the lysosomal pathway. WT as well as M98K-OPTN showed significant stabilization and increase in slow-moving forms upon MG-132 treatment (**Fig. 3C**) but only marginal change in levels was seen upon chloroquine treatment (**Fig. 3D**). These data indicate that overexpressed OPTN is processed predominantly by proteasomes.

Since M98K expression affected the turnover of cellular TFRC through the lysosomal pathway, it was important to determine the mechanism by which TFRC turnover is regulated constitutively in RGC-5 cells. Treatment of RGC-5 cells with NH_4Cl or chloroquine resulted in a concentration-dependent increase in TFRC levels (**Fig. S3A and S3B**), whereas treatment with a proteasomal inhibitor, MG-132, did not have any significant effect (**Fig. S3C**). These results suggested that endogenous TFRC is normally processed through the lysosomal pathway in RGC-5 cells as reported earlier for some other cells.[35] We also determined the localization of TFRC in cells treated with chloroquine. RGC-5 cells were incubated with Texas Red conjugated Dextran (TR-Dextran), which accumulates in lysosomes,[40] for 8 h prior to treatment with chloroquine for 18 h. Endogenous TFRC accumulated in TR-Dextran positive lysosomal compartments after chloroquine treatment (**Fig. S3D**). This result further confirmed that TFRC goes through lysosomal degradation. Treatment of RGC-5 cells with chloroquine or NH_4Cl resulted in an increase in the level of endogenous OPTN (**Fig. S3A and S3B**) whereas treatment with MG-132 showed no increase (**Fig. S3C**). These results suggest that endogenous OPTN is processed through lysosomal pathway in RGC-5 cells although overexpressed OPTN is primarily processed through the proteasomal pathway (**Fig. 3C**). Treatment of HeLa or IMR-32 cells with a lysosomal inhibitor, chloroquine, resulted in increase in levels of both endogenous TFRC as well as OPTN, whereas treatment with a proteasomal inhibitor, MG-132, showed no increase in TFRC or in OPTN levels (**Fig. S3E**).

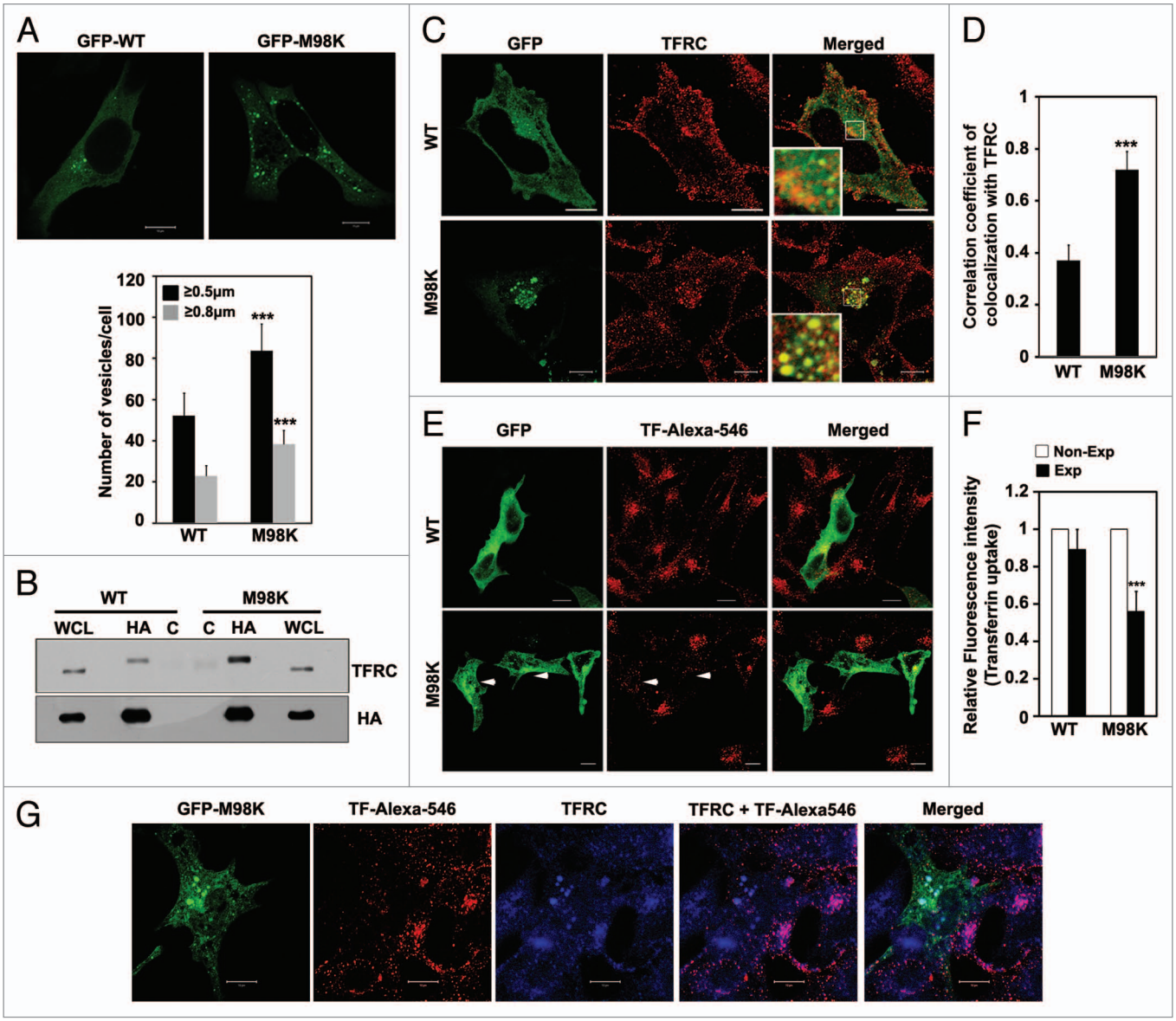

Figure 2. M98K mutant shows enhanced interaction and colocalization with TFRC compared with WT-OPTN. (**A**) M98K forms more and larger vesicles. Upper panel, confocal images of RGC-5 cells showing vesicles formed by GFP-tagged construct of WT or M98K-OPTN after 24 h of expression. Scale bar: 10 μm. Lower panel, quantitation of vesicles formed by GFP-tagged WT or M98K-OPTN after 24 h of expression, based on size. n = 100 cells, ***$p < 0.001$. (**B**) Interaction of M98K with TFRC. RGC-5 cells were infected with adenoviruses expressing HA-tagged WT or M98K-OPTN. After 6 h of infection, cells were treated with 25 μM chloroquine for 12 h and cell lysates subjected to immunoprecipitation with HA antibody (HA) or control antibody (C) and western blotting with TFRC and HA antibodies. WCL, whole cell lysates. (**C**) Representative confocal images of RGC-5 cells showing colocalization of endogenous TFRC with GFP-tagged WT or M98K-OPTN after 24 h of expression. Scale bar: 10 μm. (**D**) The graph represents correlation coefficient of colocalization between GFP-WT, or GFP-M98K and endogenous TFRC. n = 30, ***$p < 0.001$. (**E**) Effect of M98K expression on transferrin uptake. RGC-5 cells expressing GFP-tagged WT or M98K were subjected to serum starvation for 2 h and then incubated with Alexa-546 conjugated transferrin (TF-Alexa-546) for 15 min. Cells were fixed and analyzed by confocal microscopy. Scale bar: 10 μm. Arrow heads denote cells with less transferrin uptake. (**F**) Quantitation of transferrin uptake by measuring the fluorescence intensity. Data represent the uptake of labeled transferrin in WT or M98K-OPTN-expressing cells (Exp), compared with nonexpressing cells (Non-Exp). n = 150 cells ***$p < 0.001$. (**G**) Representative confocal images showing colocalization of TF-Alexa-546 with TFRC in M98K-expressing cells after 24 h of expression. Scale bar: 10 μm.

Autophagy contributes to cell death induced by M98K-OPTN. Recently, OPTN has been shown to function as an autophagy receptor through its interaction with LC3.[14] Autophagy occurs in specific cellular contexts, though the molecular components required for the phenomenon are widely expressed.[33,41,42] Our observations that M98K induces cell death selectively in RGC-5 cells, and is involved in the formation of juxta-nuclear foci prompted us to examine the possibility of M98K inducing autophagy. Conversion of the cytosolic 18 kDa LC3-I form to the cleaved and lipidated LC3-II product, which is associated with autophagosomal membranes, correlates with the extent of autophagosome formation and serves as an indicator of autophagy.

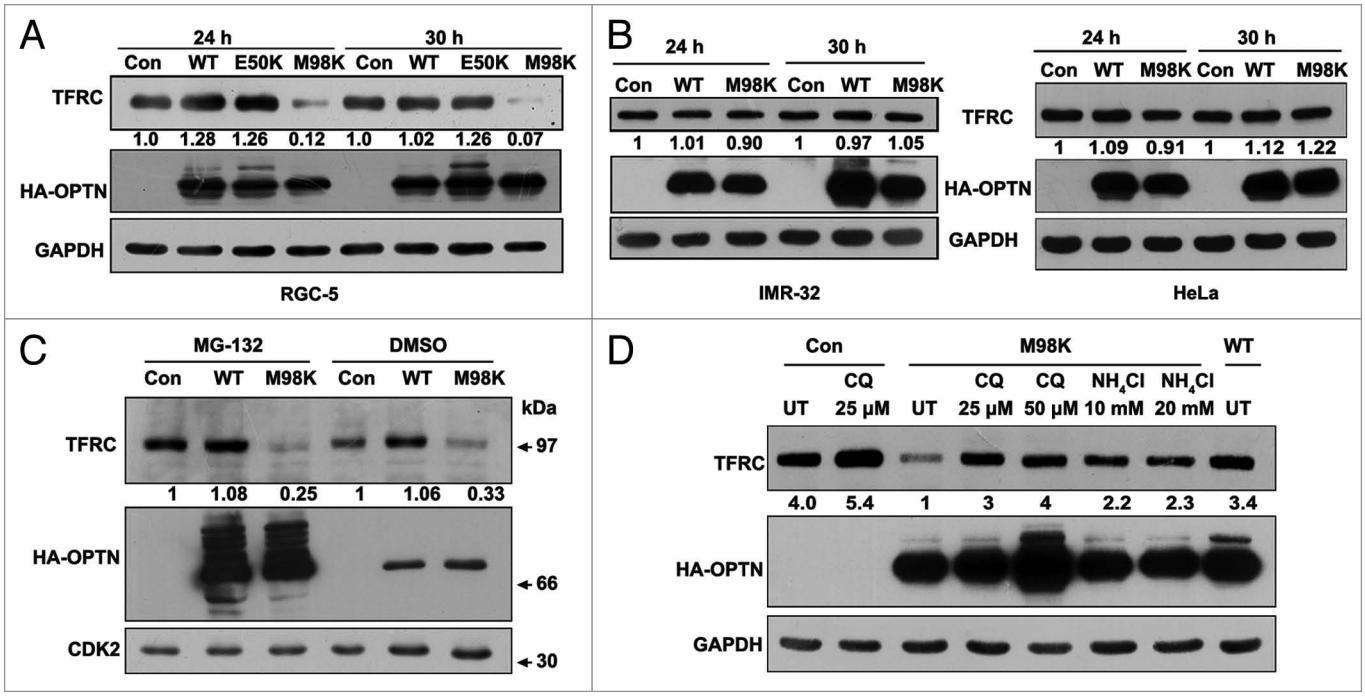

Figure 3. M98K expression induces TFRC degradation through lysosomal pathway in RGC-5 cells. (**A**) Western blot shows TFRC levels in RGC-5 cells infected with control (con), WT, E50K or M98K adenoviruses after 24 and 30 h of expression. GAPDH was used as a loading control. The numbers below TFRC blot indicate relative TFRC levels after normalization. (**B**) Effect of M98K expression on TFRC levels in IMR-32 (left panel) and HeLa (right panel) cells. (**C**) M98K-mediated TFRC degradation is independent of proteasomal degradation. RGC-5 cells infected with control (con), WT or M98K adenoviruses for 12 h were treated with either DMSO or with 5 μM MG-132 for further 12 h. Cell lysates were then subjected to western blotting. CDK2 was used as a loading control. (**D**) Effect of lysosomal inhibitors on M98K-mediated TFRC degradation. After 6 h of infection with the indicated adenoviruses, RGC-5 cells were either left untreated or treated with 25 and 50 μM of chloroquine or 10 and 20 mM of ammonium chloride for 24 h. Whole cell lysates were subjected to western blotting. CQ, chloroquine.

We observed an increase in LC3-II and GFP-MAP1LC3B (GFP-LC3B)-positive dots (autophagosomes) in M98K-expressing cells relative to control and WT-OPTN expressing cells (**Fig. 4A and B**). An increase in LC3-II isoform and autophagosome number could also be the result of a block in autophagy. To rule out this possibility, we examined the autophagy flux using the mCherry-GFP-LC3B reporter construct.[43] mCherry-GFP-LC3B is detectable in autophagosomes and also in autolysosomes but GFP fluorescence is seen only in autophagosomes and not in autolysosomes due to sensitivity of GFP to low pH in autolysosomes. We measured the autophagy flux in basal as well as amino acid starvation conditions in M98K-expressing cells. Expression of M98K significantly increased the autophagy flux in basal and autophagy-inducing conditions (**Fig. 4C and D**). To further validate the involvement of autophagy in M98K-mediated cell death, we knocked down a gene essential for autophagosome formation, *Atg5*. Knockdown of *Atg5* by shRNA significantly reduced TFRC degradation and cell death mediated by M98K in RGC-5 cells (**Fig. 4E and F**). These results suggested that overexpression of M98K induced autophagy which resulted in TFRC degradation and cell death.

Wild et al. have recently shown that mutation of Phe178 to Ala in OPTN abrogates its ability to interact with LC3.[14] To determine if M98K-induced cell death was dependent on its ability to bind LC3, we generated a double mutant of OPTN, M98K-F178A and observed that expression of this mutant caused significantly less cell death in RGC-5 compared with M98K mutant (**Fig. 4G**) indicating that autophagic processes contribute to cell death induced by M98K. Expression of the M98K-F178A mutant did not induce CASP3 and PARP1 cleavage (**Fig. 1F**). LC3B-positive intracellular structures have been characterized as autophagosomes.[44,45] M98K-OPTN showed significantly higher colocalization with GFP-LC3B compared with WT-OPTN in vesicular structures likely to be autophagosomes (**Fig. 4H and I**). The double mutant M98K-F178A showed significantly lesser colocalization with GFP-LC3B, indicating that this mutant is compromised in its ability to interact with autophagosomes. M98K-F178A double mutant was also less effective in its ability to degrade TFRC as compared with M98K mutant (**Fig. 4J**) suggesting that autophagy is involved in M98K-mediated TFRC degradation. M98K showed very little colocalization with lysosomal markers LAMP1 and TR-Dextran in RGC-5 cells (**Fig. S4A and S4B**). The colocalization of M98K with lysosomal markers is much lower than that observed with the autophagosomal marker LC3 (**Fig. 4H and I**).

Our results suggested that M98K colocalizes with autophagosomes and causes lysosomal degradation of TFRC. Therefore, we examined the possibility of endogenous TFRC localizing to autophagosomes in M98K-expressing cells. M98K-expressing cells showed localization of TFRC in

GFP-LC3B-positive structures, which were also positive for M98K (**Fig. 5A**). WT-OPTN showed a lower number of such structures positive for GFP-LC3B and TFRC. Compared with WT-OPTN, M98K foci showed significantly better colocalization of TFRC with GFP-LC3B (**Fig. 5B**). These results indicate that M98K-OPTN potentiates delivery of TFRC to autophagosomes for degradation.

We also examined whether cellular TFRC colocalizes with autophagosomes upon induction of autophagy by amino acid and growth factor starvation. We found enhanced colocalization of TFRC in GFP-LC3B-positive structures under condition of autophagy induction (**Fig. 5C**). TFRC also showed good colocalization with endogenous LC3 in chloroquine-treated cells (**Fig. 5D**). Endogenous OPTN also colocalized partially with GFP-LC3B-positive structures (**Fig. 5E**) suggesting the presence of OPTN in autophagosomes. Autophagy induction by EBSS reduced TFRC level in RGC-5 cells in a time-dependent manner (**Fig. 5F**). We also observed change in OPTN levels under these conditions (**Fig. 5F**). We further examined the effect of EBSS on M98K-induced cell death at various time points. EBSS treatment increased cell death with time compared with untreated conditions (**Fig. 5G**). We also examined the effect of EBSS on M98K-mediated TFRC degradation. Amino acid starvation significantly increased M98K-mediated TFRC degradation (**Fig. 5H**). Autophagy inducing conditions, therefore, enhanced M98K-mediated effects.

Coexpression of TFRC or inhibition of its degradation prevents M98K-induced cell death. Our results showed reduction in TFRC levels and transferrin uptake in M98K-expressing cells, suggesting that compromise in cellular TFRC function may be responsible for cell death induced by M98K. Therefore, we examined if TFRC overexpression could complement and inhibit cell death induced by M98K. A significant reduction in cell death was observed in cells coexpressing TFRC with M98K (**Fig. 6A**). Expression of TFRC alone did not induce death in RGC-5 cells. TFRC expression did not affect M98K expression (**Fig. 6B**). We also checked whether inhibition of TFRC degradation by a lysosomal inhibitor could rescue cells from death induced by M98K. Treatment with 10 or 25 μM chloroquine for 24 h rescued cells from M98K-induced death significantly (**Fig. 6C**). Treatment with chloroquine for 24 h inhibited M98K-induced CASP3 and PARP1 cleavage (**Fig. 1F**). Decreased TFRC levels and reduced transferrin uptake would eventually lead to less iron uptake which could be the cause of cell death induced by M98K. To test if iron supplementation could inhibit cell death, RGC-5 cells transfected with M98K were treated with an iron donor, ferric ammonium citrate, for 24 h. Iron supplementation resulted in inhibition of cell death induced by M98K expression (**Fig. 6D**) or M98K expression and EBSS treatment (**Fig. 6E**). These results suggest that M98K overexpression interferes with the maintenance of TFRC levels which is necessary to regulate iron homeostasis and survival of RGC-5 cells.

Functional ubiquitin binding domain of OPTN is required for M98K-induced TFRC degradation and cell death. Functional UBD of OPTN is required for trafficking of TFRC to the perinuclear region, interaction with TFRC and also for autophagic response to *Salmonella*.[14,15] A functional UBD is also required for E50K mediated cell death in RGC-5 cells.[15] The requirement of a functional UBD in determining the properties of the M98K mutant of OPTN was examined by introducing a second mutation (D474N) in the UBD that disables ubiquitin binding. Overexpression of M98K-D474N in RGC-5 cells showed significantly less cell death compared with M98K (**Fig. 7A**). M98K-D474N mutant did not induce CASP3 and PARP1 cleavage (**Fig. 1F**). The M98K-D474N double mutant showed cytosolic localization with no foci formation, and reduced colocalization with TFRC (**Fig. 7B**) and GFP-LC3B (**Fig. 7C**). Reduced formation of autophagosomes (GFP-LC3B-positive structures) by the M98K-D474N mutant might be due to loss of interaction with a ubiquitinated protein that facilitates its recruitment to autophagosomes. Unlike M98K, the double mutant, M98K-D474N, did not cause any increase in autophagy flux (**Fig. 4C and D**). Adenoviral overexpression of M98K-D474N did not cause reduction in TFRC levels, as did M98K (**Fig. 7D**). These results suggested that functional UBD is required for M98K-induced degradation of TFRC and death of RGC-5 cells.

Role of RAB12 in M98K-induced cell death. Our results so far have shown that M98K causes degradation of TFRC leading to death of RGC-5 cells. How does M98K-OPTN mediate this process? Recently it has been shown that TFRC is constitutively

Figure 4 (See opposite page). M98K expression induces autophagy. (**A**) Effect of M98K expression on LC3-II levels. Western blot shows LC3-II levels in RGC-5 cell lysate after 24 h of adenovirus mediated expression of control (con), WT or M98K. GAPDH was used as a loading control. (**B**) Effect of M98K expression on autophagosome formation. Data represent the number of GFP-LC3B dots (autophagosomes) per cell in control (con), WT or M98K-expressing cells after 24 h of transfection. n = 45 cells ***p < 0.001. (**C**) RGC-5 cells were transfected with either control plasmid, HA-M98K or HA-M98K-D474N along with mCherry-GFP-LC3B construct for 24 h and were either kept untreated (upper panel) or in amino acid and serum-free media (EBSS) for 2 h (lower panel). Representative merged confocal images show autophagosomes (yellow dots) and autolysosomes (red dots only). (**D**) Quantitation of number of autophagosomes (green dots) and red dots per cell in control, HA-M98K or HA-M98K-D474N transfected in untreated (left panel) and EBSS treated (2 h) cells (right panel). n = 40 cells, ***p < 0.001; **p < 0.01; *p < 0.05. (**E**) Knockdown of *Atg5* reduces M98K-mediated TFRC degradation. RGC-5 cells were transfected with either Con-Sh, *Atg5*-ShA or *Atg5*-ShB and after 24 h of knockdown, were either infected with WT or M98K adenoviruses for 24 h. Cell lysates were subjected to western blotting. GAPDH was used as a loading control. The numbers below TFRC and ATG5 blots indicate relative TFRC and ATG5 levels after normalization. (**F**) Knockdown of ATG5 reduced M98K-induced cell death. Data represent quantitation of cell death induced by M98K with or without *Atg5* knockdown. n = 6, ***p < 0.001. (**G**) Effect of LC3 binding-defective mutation in M98K on cell death induced by M98K. Data show quantitation of cell death upon expression of M98K or M98K-F178A. n = 6 experiments ***p < 0.001. (**H**) Colocalization of GFP-LC3B with WT, M98K or their LC-3 binding deficient mutants. Panels show representative confocal images of RGC-5 cells expressing GFP-LC3B with indicated OPTN mutants. Scale bar: 10 μm. Magnified areas are shown as insets. (**I**) The graph shows correlation coefficient of colocalization of LC3B with indicated constructs of OPTN. n = 30 cells, ***p < 0.001. (**J**) Effect of M98K and LC3 binding-defective mutation in M98K, M98K-F178A, on endogenous TFRC levels after 32 h of transfection. Western blot showing TFRC levels upon expression of WT, M98K and M98K-F178A. GAPDH was used as a loading control.

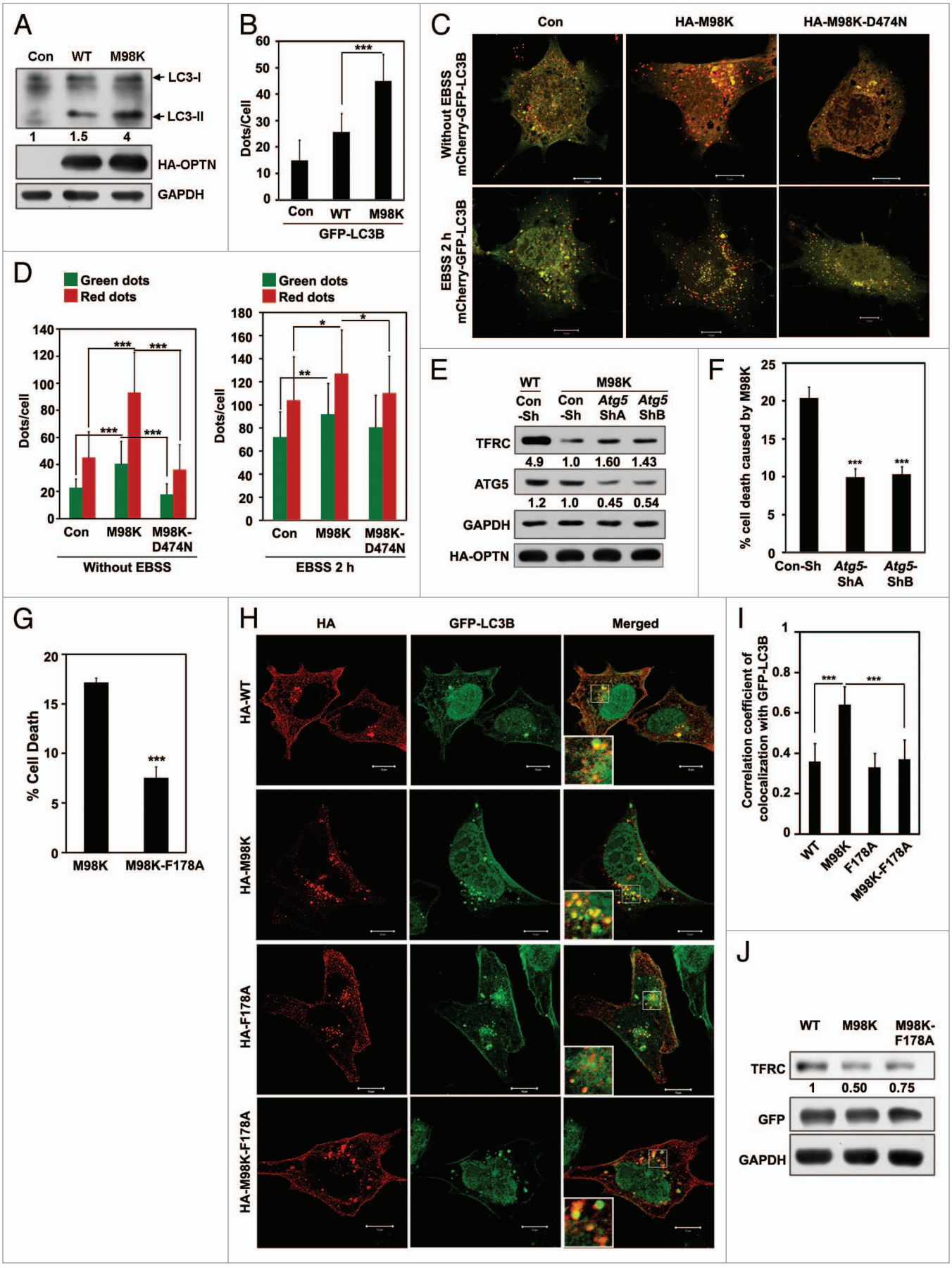

degraded in lysosomes involving RAB12 mediated trafficking of TFRC from recycling endosomes to lysosomes.[35] Therefore, we examined the role of RAB12 in M98K-induced death of RGC-5 cells using RNAi-mediated knockdown. Knockdown of *Rab12* using two plasmid constructs expressing shRNA, ShA and ShB, resulted in reduction in M98K-induced death of RGC-5 cells (**Fig. 8A and B**). Knockdown of *Rab12* resulted in enhanced level of endogenous TFRC and LC3-II in RGC-5 cells (**Fig. 8C**). M98K-induced degradation of TFRC was reduced upon knockdown of *Rab12* (**Fig. 8D**). M98K showed significantly higher colocalization with overexpressed RAB12 as compared with WT-OPTN (**Fig. 8E**). Endogenous OPTN also showed partial colocalization with GFP-RAB12 (**Fig. 8F**). Interaction of RAB12 with OPTN was examined in cell lysates using an immunoprecipitation assay. RAB12 could co-immunoprecipitate OPTN, and M98K showed a marginal increase in this interaction (**Fig. 8G**). Taken together, these results suggest that M98K promotes RAB12-mediated degradation of TFRC which is responsible for death of RGC-5 cells. We also examined whether RAB12 directly interacted with OPTN and its mutant M98K by yeast two-hybrid assay. We did not observe any direct interaction between RAB12 and WT-OPTN or M98K as there was no growth on selection media (**Fig. S2C**).

Role of RAB12 in autophagy. M98K-induced cell death is dependent on autophagy and also requires RAB12 function. This raised the possibility of involvement of RAB12 in autophagy. To explore this possibility, we examined the colocalization of RAB12 with autophagosomes. Overexpressed RAB12 showed localization to GFP-LC3B-positive autophagosomes (**Fig. 8H**). RAB12 also showed colocalization with endogenous LC3-positive structures in chloroquine-treated cells (**Fig. 8I**). We examined the colocalization of RAB12 and cellular TFRC in autophagosomes. It was observed that endogenous TFRC was present in GFP-LC3B-positive structures along with RAB12 (**Fig. S5**). Overall, our results suggested that RAB12 is present in autophagosomes and it plays a crucial role in autophagic death of RGC-5 cells induced by M98K variant of OPTN. What is the role of RAB12 in autophagy? We examined the role of RAB12 in the formation of autolysosomes which are produced upon fusion of autophagosomes with lysosomes. Using the reporter construct, mCherry-GFP-LC3B, we examined the role of RAB12 in autophagosome and autolysosome formation under basal and amino acid starvation-induced autophagic conditions. Knockdown of *Rab12* resulted in reduced formation of autolysosomes (only red dots) in basal (**Fig. 9A and C**) and autophagy-inducing conditions (**Fig. 9B and D**).

Discussion

Glaucoma is a neurodegenerative eye disease where there is progressive loss of vision due to death of retinal ganglion cells.[3] Mutations in OPTN have been implicated in glaucoma pathogenesis, primarily in NTG, a subtype of POAG. In the original paper describing OPTN as a candidate gene for POAG, it was proposed that M98K variant of OPTN is strongly associated with NTG.[1] Though there were conflicting findings on the association of M98K polymorphism with glaucoma by various investigators, meta-analysis studies suggest that there is a significant, but weak association between M98K and glaucoma in some Asian populations.[4,8-10] It is, therefore, important to understand how this mutation alters OPTN function at the cellular level. Our results showed that M98K expression causes death of RGC-5 cells selectively, as other neuronal and non-neuronal cell lines tested were not affected. M98K-induced cell death was not inhibited by the antiapoptotic protein BCL2 or antioxidants. The E50K mutant of OPTN has been shown to cause oxidative stress-mediated apoptosis-like death of retinal ganglion cells that is inhibited by BCL2. The E50K mutant causes altered interactions with RAB8A,[15,30,32] but M98K mutant does not. It therefore appears that E50K and M98K mutations result in engagement of different effectors in signaling to cell death. The extent of cell death induced by these two variants also differs, with M98K being less potent than E50K.

Our present study showed that M98K overexpression caused degradation of TFRC selectively in RGC-5 cells. Cellular TFRC is normally processed through lysosomal degradation pathway in RGC-5 cells. We have seen that degradation of TFRC upon M98K overexpression was also through lysosomal pathway and not by proteasomal pathway. Treatment of cells with a lysosomal inhibitor or overexpression of TFRC rescued from M98K-mediated cell death. These results suggest that decrease in the TFRC levels is the major cause for cell death by M98K. This is in corroboration with cell death specificity in RGC-5 cells by M98K as TFRC levels were not reduced in other cell lines tested in the presence of M98K. Regulation of iron homeostasis is very critical, particularly in neuronal cells. Misregulation of iron homeostasis is associated with adult neurodegeneration.[46-48] *Tfrc* knockout mice die before embryonic day 12.5 and the

Figure 5 (See opposite page). M98K-OPTN enhances TFRC localization in autophagosomes. (**A**) TFRC colocalizes with GFP-LC3B positive structures in M98K-expressing cells. Panels show representative confocal images of RGC-5 cells expressing GFP-LC3B with HA-WT or HA-M98K OPTN, and costained for endogenous TFRC. Scale bar: 10 μm. Magnified areas are shown as insets. (**B**) The graph shows correlation coefficient of colocalization between GFP-LC3B and endogenous TFRC in WT or M98K-OPTN expressing cells. (**C**) Autophagy induction increases the localization of TFRC to GFP-LC3B positive structures. Panels show representative images of RGC-5 cells expressing GFP-LC3B with cellular TFRC grown in serum-containing media (UT) or in amino acid- and serum-free media (EBSS) for 3 h. Magnified areas are shown as insets. (**D**) Colocalization of cellular TFRC with endogenous LC3 in chloroquine (25 μM for 8 h) treated cells. (**E**) Colocalization of endogenous OPTN with GFP-LC3B-positive structures. Scale bar: 10 μm. (**F**) Induction of autophagy reduces TFRC levels. RGC-5 cells were either kept untreated or treated with EBSS for the indicated time. Western blots show levels of TFRC and endogenous OPTN. GAPDH is a loading control. The numbers below TFRC and OPTN blots indicate relative TFRC and OPTN levels after normalization. (**G**) Induction of autophagy enhances M98K-mediated cell death in a time-dependent manner. RGC-5 cells transfected with GFP-M98K were either kept untreated or were treated with EBSS for 2 h after indicated time of expression. Data represent cell death mediated by GFP-M98K in untreated and EBSS treated conditions. n = 3 experiments. ***$p < 0.001$. **$p < 0.01$. (**H**) Western blot shows TFRC levels in control and M98K-infected RGC-5 cells in untreated and EBSS treated conditions. The numbers below TFRC blot indicate relative TFRC levels after normalization.

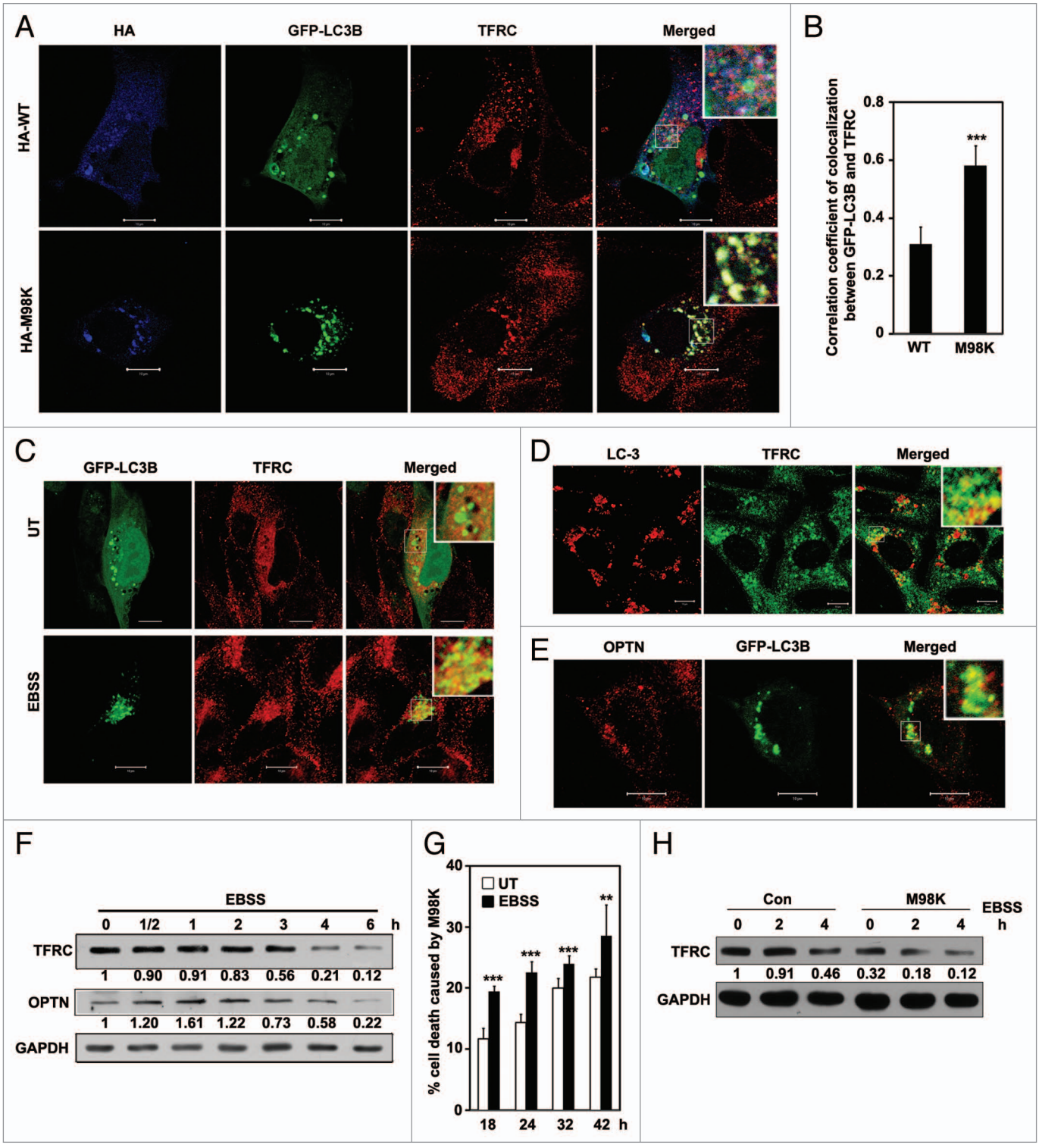

Figure 5. For figure legend, see page 518.

knockout embryos show defects in nervous and hematopoietic systems. Increased apoptosis was seen in neural tissue but not in non-neural tissues of *Tfrc* knockout embryos.[46] Thus, TFRC has a unique function in neural and hematopoietic systems. Our results suggest that TFRC function is critical for the survival of retinal ganglion cells, and impaired TFRC function contributes to M98K-induced death of RGC-5.

Autophagy is a conserved mechanism for degradation of damaged proteins, organelles and protein aggregates.[41] This degradation occurs when double membrane-bound structures known as

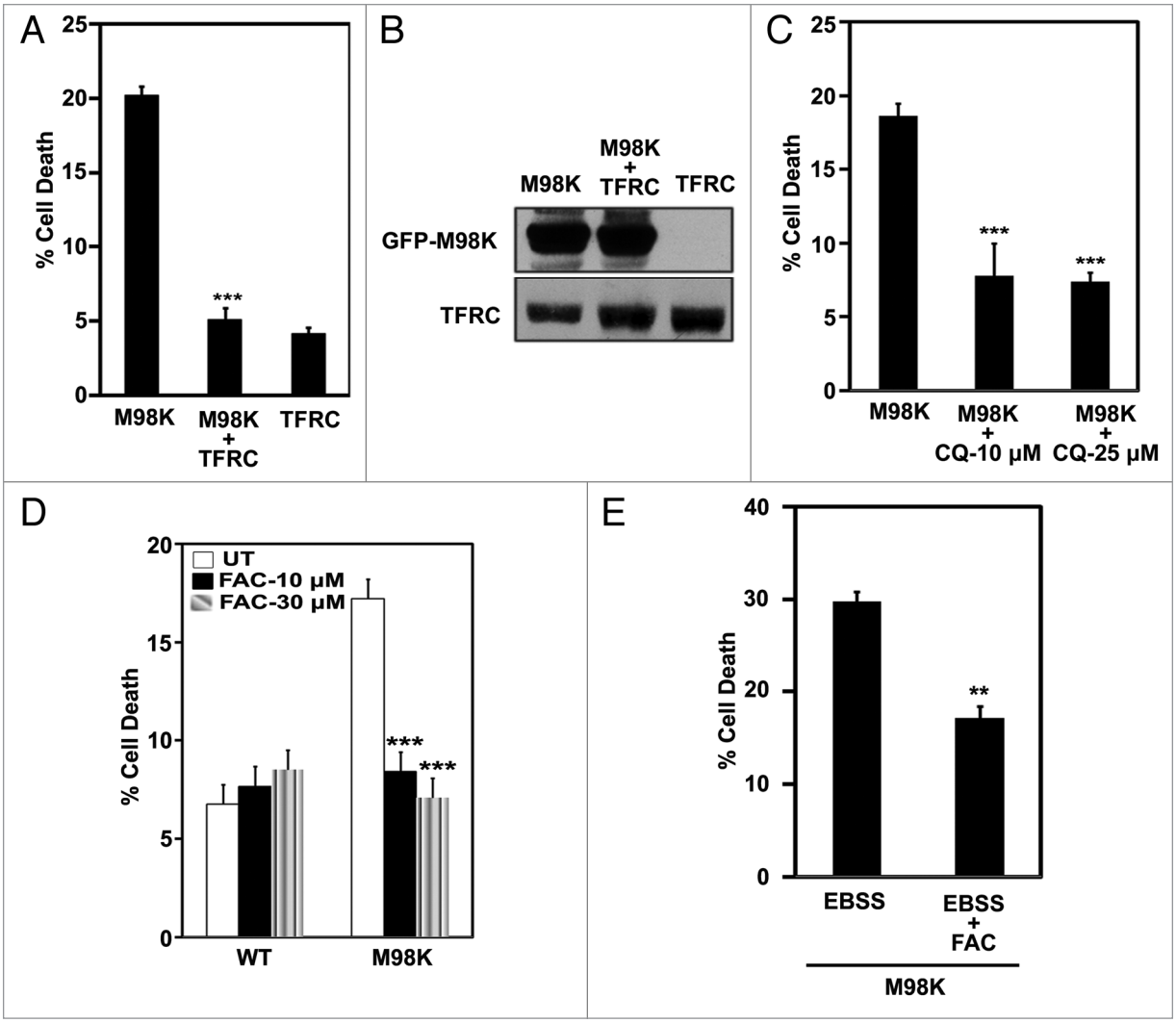

Figure 6. Restoration of TFRC levels reduces M98K-induced cell death. (**A**) Effect of TFRC coexpression on M98K-induced cell death. Data represent mean ± s.d of percentage of expressing cells showing apoptotic morphology upon 32 h of expression. n = 6, ***p < 0.001. (**B**) Western blot shows M98K protein levels in the presence or absence of coexpressed TFRC. (**C**) Quantitation of cell death induced by M98K in the presence of chloroquine in RGC-5 cells. n = 6, **p < 0.001. CQ, chloroquine. (**D**) Quantitation of cell death induced by M98K in the presence of FAC, an iron supplement. n = 6 experiments, ***p < 0.001. FAC, ferric ammonium citrate; UT, untreated. (**E**) Quantitation of cell death induced by M98K with 4 h of EBSS treatment with or without FAC (30 μM, 24 h). ***p < 0.001.

autophagosomes fuse with lysosomes to form autolysosomes. The cleaved and lipid-conjugated form of LC3 (LC3-II) is tightly associated with the phagophore and autophagosomal membrane and serves as an autophagy marker. Cargo-selective autophagy is thought to be mediated by receptor proteins that link specific cargo proteins to LC3.[49-51] OPTN was recently identified as an autophagy receptor that directly binds to LC3.[14] Mutational inactivation of LC3-binding site or UBD, results in inactivation of autophagic function of OPTN.[14] Our results suggest that M98K-induced RGC death involves autophagic signaling because knockdown of *Atg5* or mutation of the LC3-binding site in M98K inhibits its ability to induce cell death and TFRC degradation. An enhanced level of the LC3-II isoform seen in M98K-expressing cells and localization of TFRC to GFP-LC3B-positive structures provide additional evidence for activation of autophagic signaling. Our results suggest that M98K is a gain-of-function mutation, which shows enhanced autophagic signaling leading to TFRC degradation and cell death. This increased autophagy does not clear overexpressed M98K-OPTN, as it is cleaved mainly by proteasomal degradation.

Autophagosomes are membranous structures which can originate from the ER, mitochondria, plasma membrane, Golgi apparatus, early endosome, recycling endosome, etc.[52,53] Recent studies have shown that transferrin receptor-positive recycling endosomes contribute to autophagosome formation during starvation-induced autophagy.[54] Our results suggest that M98K-OPTN potentiates the delivery of TFRC to autophagosomes. M98K-OPTN might be inducing an autophagic pathway originating from TFRC-positive recycling endosomes that leads to TFRC degradation.

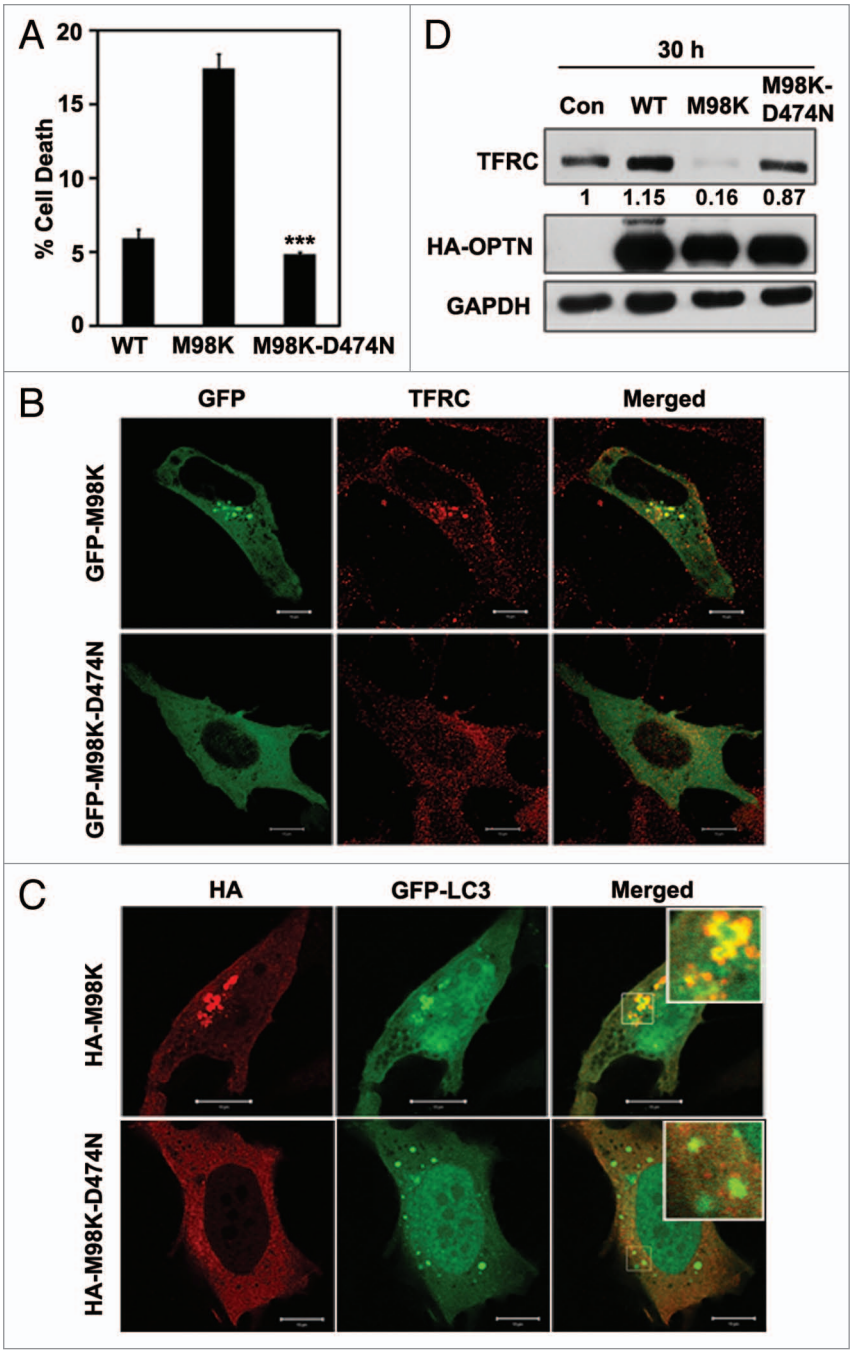

Figure 7. TFRC degradation and cell death induced by M98K are dependent on its UBD. (**A**) Quantitation of cell death induced by WT, M98K and M98K-D474N (ubiquitin binding-defective mutant of M98K) in RGC-5 cells. n = 6, ***p < 0.001. (**B**) Representative confocal images showing colocalization of M98K and M98K-D474N mutants with TFRC. Scale bar: 10 μm. (**C**) Representative confocal images showing colocalization of M98K and M98K-D474N mutants with GFP-LC3B. Scale bar: 10 μm. (**D**) Western blots show levels of TFRC in RGC-5 cells after adenovirus-mediated expression of control (con), WT, M98K and M98K-D474N. GAPDH was used as a loading control.

Constitutive degradation of TFRC occurs in lysosomes and requires RAB12-mediated function.[35] It has been suggested that RAB12 mediates trafficking of TFRC from recycling endosomes to lysosomes. We have seen that knockdown of *Rab12* increases TFRC levels and also reduces M98K-induced cell death in RGC-5. Since autophagy is involved in M98K-induced death of RGC-5 cells, RAB12 is likely to have a role in autophagy. This hypothesis is supported by the following observations. (1) RAB12 colocalizes with the autophagy receptor OPTN and forms a complex with it; (2) M98K shows increased colocalization with RAB12, and RAB12 is required for M98K-induced autophagic cell death; (3) RAB12 shows colocalization with GFP-LC3B as well as endogenous LC3-positive structures (autophagosomes); and (4) *Rab12* knockdown causes a reduction in autolysosomes induced by basal as well as nutrient-starved conditions. Overall our results suggest that M98K-OPTN enhances RAB12-dependent constitutive degradation of TFRC by autophagosomes that leads to death of RGC-5 cells.

M98K-OPTN-induced death of RGC-5 cells shows features of apoptosis (chromatin condensation, shrinkage of cytoplasm, CASP3 cleavage) and it involves autophagy. The relationship between apoptosis and autophagy, in general, is quite complex.[55,56] Autophagy can cause cell death or prevent cell death by apoptosis, depending upon the inducer and cellular context. Autophagy can also occur along with apoptosis in a coordinated manner without being a cause of apoptosis. Autophagy is required for M98K-induced apoptotic death of RGC-5 cells, as shown by reduction of apoptosis upon knockdown of *Atg5* or mutation of LC3-binding site in M98K-OPTN. However, the molecular connection between M98K-induced autophagy and apoptosis is not clear, although autophagic TFRC degradation contributes to apoptosis.

M98K-OPTN induces TFRC degradation and death of RGC-5 cells selectively, indicating relevance to disease pathogenesis. However, what determines this cell type selectivity of M98K-OPTN is not clear. Autophagic degradation of TFRC, which occurs specifically in RGC-5 cells, plays a crucial role in death induced by M98K. Therefore, M98K is likely to be activating a signaling event that causes or enhances autophagic degradation of TFRC in RGC-5. An understanding of the details of molecular mechanisms of autophagy in retinal ganglion cells might provide an insight into cell type specificity of M98K-induced TFRC degradation and cell death.

In conclusion, our results show that M98K mutation causes a functional defect in OPTN leading to selective death of RGC-5 cells. This variant primarily interferes with maintenance of

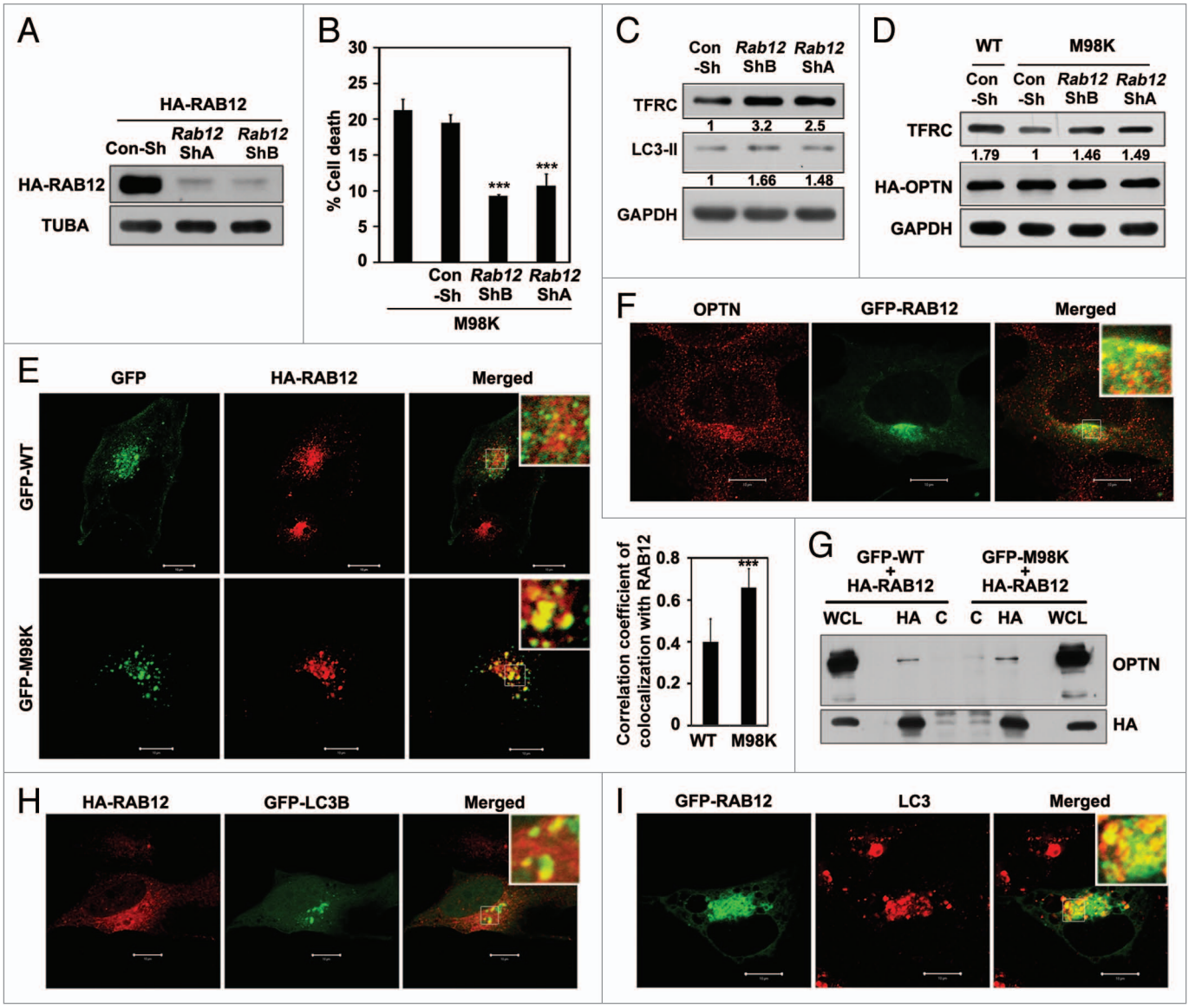

Figure 8. Role of RAB12 in M98K-induced death of RGC-5 cells. (**A**) Western blot shows knockdown of HA-RAB12 by *Rab12* shRNAs, ShA and ShB in RGC-5 cells. Tubulin was used as a loading control. Con-Sh, Control shRNA; TUBA, α-tubulin. (**B**) Knockdown of *Rab12* reduced M98K-mediated cell death. Data represent quantitation of cell death induced by M98K with or without knockdown of *Rab12*. n = 6, ***p < 0.001. (**C**) Western blots show endogenous levels of TFRC and LC3-II after knockdown of *Rab12* for 48 h by *Rab12* ShB and ShA. GAPDH was used as a loading control. (**D**) Effect of *Rab12* knockdown on TFRC degradation by M98K. RGC-5 cells were transfected with either Con-Sh or *Rab12* ShB or ShA and after 24 h of knockdown, were infected with either WT or M98K adenoviruses for 24 h. Cell lysates were subjected to western blotting. GAPDH was used as a loading control. (**E**) Left panel, Representative confocal images showing colocalization of M98K and WT with HA-RAB12. Magnified areas are shown as insets. Scale bar: 10 μm. The graph on the right represents correlation coefficient of colocalization of WT or M98K with RAB12. n = 30 cells, ***p < 0.001. (**F**) Colocalization of endogenous OPTN and GFP-RAB12. Scale bar: 10 μm. (**G**) Interaction of OPTN with overexpressed RAB12. Cell lysates of RGC-5 cells expressing WT or M98K with HA-RAB12 were immunoprecipitated using HA (IP) or control antibody (C) and subjected to western blotting with HA and OPTN antibodies. WCL, whole cell lysates. (**H**) Colocalization of HA-RAB12 with GFP-LC3B positive structures. (**I**) Colocalization of GFP-RAB12 with endogenous LC3 in chloroquine (25 μM for 8 h) treated cells. Scale bar: 10 μm.

cellular TFRC levels and engages RAB12 to cause its autophagic degradation, rather than enable its recycling back to cell membrane (**Fig. 10**). We suggest that M98K enables a gain of function by interacting better with TFRC and causes its degradation by autophagosomes by enhanced recruitment of RAB12. TFRC is the first example of a protein cargo for OPTN that is subjected to autophagosomal degradation.

Materials and Methods

Cell culture and transfections. RGC-5, IMR-32, Cos-1 and HeLa cells were grown as monolayers in Dulbecco's Modified Eagle's Medium (DMEM) supplemented with 10% FCS, 100 μg/ml penicillin and 100 μg/ml streptomycin in a humidified atmosphere of 5% CO_2 at 37°C. Transfections were

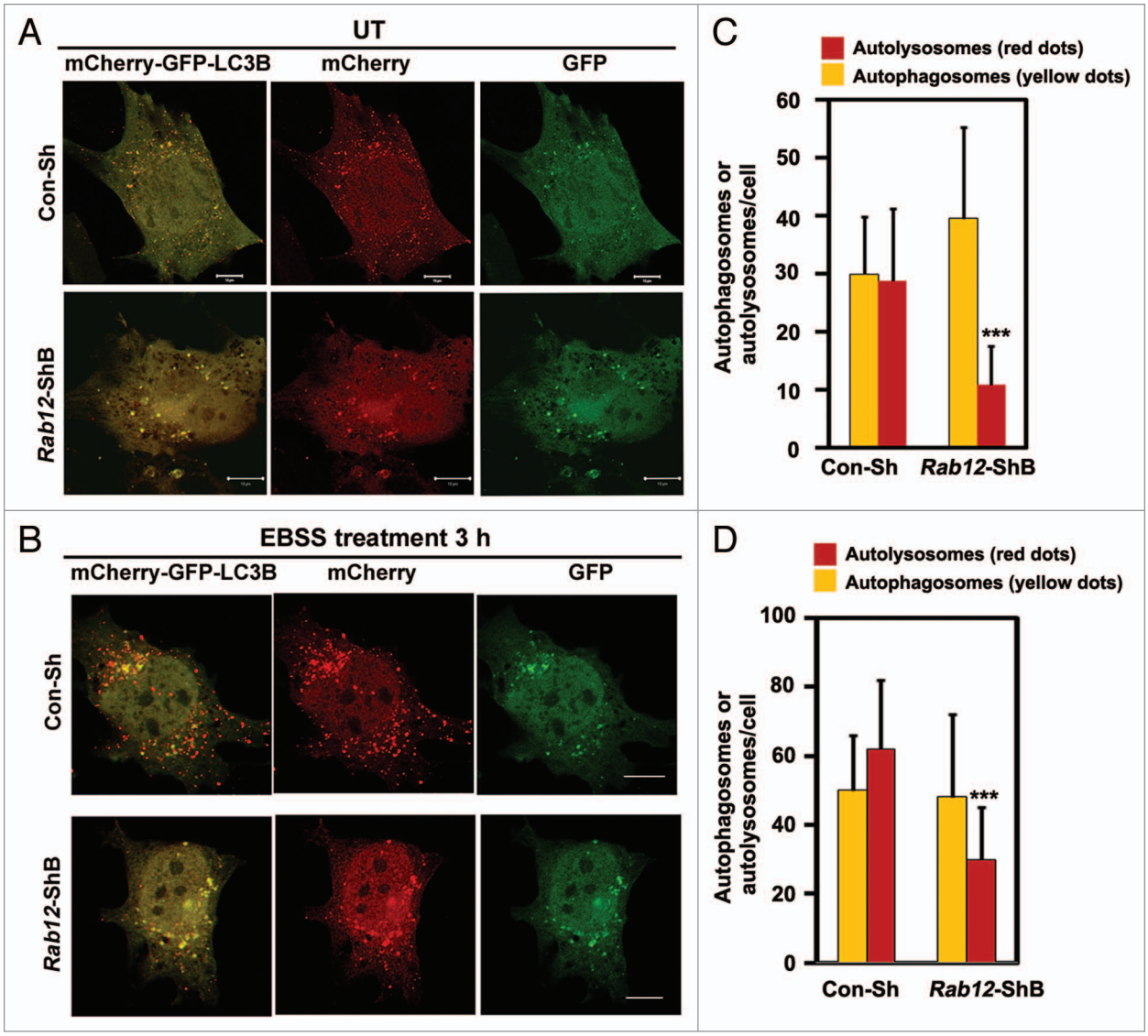

Figure 9. Knockdown of *Rab12* decreases autolysosome formation. Representative confocal images showing number of autophagosomes (yellow dots) and autolysosomes (red dots only) upon *Rab12* knockdown by control shRNA (Con-Sh) or *Rab12* shRNA, shB in untreated conditions (**A**) and in amino acid and serum-starved conditions (**B**). RGC-5 cells were transfected with either Con-Sh or *Rab12*-ShB along with mCherry-GFP-LC3B construct for 32 h and kept untreated or in EBSS media for 3 h. Quantification of number of autophagosomes (yellow dots) and autolysosomes (red dots only) per cell in control or *Rab12* knockdown cells in untreated (**C**) and in amino acid- and serum-starved conditions (**D**). n = 50 cells, ***p < 0.001.

performed on cells grown as a monolayer using Lipofectamine (Invitrogen, 18324-012) and Lipofectamine PLUS™ (Invitrogen, 11514-015) reagents or Lipofectamine 2000 (Invitrogen, 1168-019) according to the manufacturer's instructions. Starvation was induced by washing cells with PBS three times and incubating in Earle's Balanced Salt Solution (EBSS) media (Invitrogen, 14155063) at 37°C for the required time.

Expression vectors. Plasmid vectors for expressing human OPTN and its mutant (E50K) with HA-tag have been described.[28] HA-M98K, HA-T202R, HA-E322K, HA-M98K-D474N, HA-F178A and HA-M98K-F178A mutants were made by site-directed mutagenesis from HA-OPTN following the protocol described in QuikChange Site-Directed Mutagenesis Kit (Stratagene/Agilent). M98K, M98K-D474N, F178A and M98K-F178A were cloned in pEGFP-C3 (Clontech, 6082-1) to produce GFP-tagged OPTN mutants. Mutant CASP1- and CASP9-expressing vectors have been described earlier.[57] A SOD2-expressing vector has been described earlier.[28] cDNAs of human and mouse transferrin receptors were amplified by RT-PCR using RNA from HeLa and RGC-5 cells, respectively, and cloned in pcDNA3. Mouse *Rab12* was amplified by RT-PCR using RNA from RGC-5 cells and cloned in pcDNA3.1 and EGFP vectors. Mouse *Atg5* was amplified by RT-PCR using RNA from RGC-5 cells and cloned in pcDNA3.1. The plasmids, pdest GFP-LC3B and mCherry-GFP-LC3B were kindly provided by Dr. Terje Johansen (University of Tromsø).[43] Adenoviral vectors expressing wild-type OPTN and its E50K mutant have been described earlier.[20] Similarly, M98K and

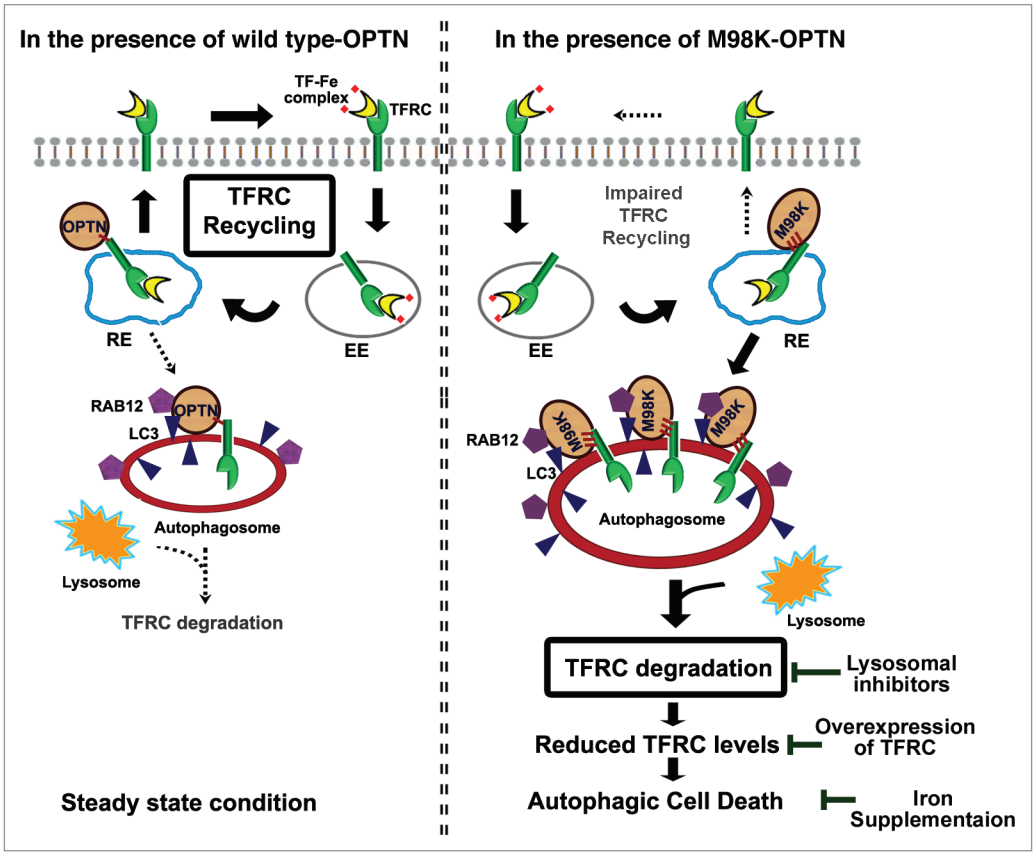

Figure 10. Model depicting how M98K variant of OPTN alters cellular transferrin receptor dynamics leading to autophagic death in RGC-5 cells. Under steady-state conditions, membrane TFRC bound to transferrin-Fe complex is internalized by endocytosis and recycled back to the plasma membrane after intracellular release of Fe. A proportion of TFRC is degraded by lysosomes. OPTN interacts with LC3 and its role as an autophagy receptor has been proposed. In the presence of M98K-OPTN, cellular TFRC turnover dynamics is altered as this variant interacts more strongly with TFRC, and enhances its localization in autophagosomes. M98K-OPTN recruits RAB12, a GTPase involved in TFRC degradation, more efficiently. As a consequence, cellular TFRC is rapidly degraded in lysosomes, rather than being recycled to the plasma membrane through recycling endosomes. Reduced cellular TFRC level causes death of RGC-5 cells that can be prevented by expression of TFRC or inhibition of TFRC degradation or iron supplementation.

M98K-D474N double mutant of OPTN adenoviral vectors were generated.[20]

Construction of vectors expressing shRNAs. Plasmid vectors for expressing shRNAs directed against mouse *Rab12* (ShA and ShB) were constructed using a U6 promoter-based vector (pmU6) as described previously.[58-60] The mouse *Rab12* sequence targeted by ShA was from nucleotides 338 to 356 and the sequence targeted by ShB was from 288 to 306 (GenBank™ accession NM_024448.2). A vector expressing shRNA of unrelated sequence (Con-Sh) of the same length was used as a control. The mouse *Atg5* sequence targeted by by ShA was from nucleotides 746 to 764 and the sequence targeted by ShB was from 459 to 477 (GenBank™ accession NM_053069.5).

Antibodies and reagents. Mouse monoclonal anti-ubiquitin (Calbiochem, CC37), rabbit polyclonal anti-OPTN (Abcam, ab23666), rabbit polyclonal LAMP1 antibody (Abcam, ab24170), mouse monoclonal anti-TFRC antibody (Zymed, 136800), rabbit polyclonal cleaved CASP3 (Asp-175) antibody (Cell Signalling Technology, 9664), rabbit polyclonal ATG5 antibody (Cell Signalling Technology, 8540), rabbit polyclonal PARP1 antibody (Roche Applied Biosystems, 11835238001), mouse monoclonal anti-HA (Roche Applied Biosystems, 11583816001), rabbit polyclonal anti-HA (Santa Cruz, sc-805), anti-CDK2 (Santa Cruz, sc-748), rabbit polyclonal and mouse monoclonal anti-GFP (Santa Cruz, sc-9996, sc-8334), normal mouse IgG (Santa Cruz, sc-2025), normal rabbit IgG (Santa Cruz, sc-2027), mouse monoclonal anti-TUBA (α-tubulin) antibody (Santa Cruz, sc-5286), anti-GAPDH (Millipore, MAB374), anti-actin (Millipore, MAB1501), Alexa-546-conjugated transferrin (Molecular Probes, T23364), Texas Red conjugated Dextran (Molecular Probes, D1846), mouse anti-LC3 antibody (Enzo Life sciences, ALX80308), rabbit anti-LC3 antibody (Cell Signalling Technology 4108), Cy-3-conjugated anti-mouse IgG (Amersham, PA43002), Cy-3-conjugated anti-rabbit IgG (Amersham, PA43004), HRP conjugated anti-mouse IgG (Amersham, NA9310), HRP conjugated anti-rabbit IgG (Amersham, NA934), Alexa-488 anti-mouse and anit-rabbit IgG (Molecular Probes, A21202, A21206), Alexa-633 conjugated anti-mouse and anti-rabbit IgG (Molecular Probes, A21050, A21070) antibodies are all commercially available. Protein

A/G agarose beads were from Santa Cruz, sc-2003. MG-132 (Calbiochem, 474790), Ammonium chloride (Sigma, A0171), chloroquine (Sigma, C6628), N-acetylcysteine (Sigma, A9165) and ferric ammonium citrate (Sigma, F5879) are commercially available.

Indirect immunofluorescence and confocal microscopy. Cells grown as monolayers on coverslips were transfected with the required plasmids. After indicated time, cells were fixed with 3.7% formaldehyde and then stained with appropriate antibodies. Cells were fixed with methanol for staining endogenous LC3. Indirect immunostaining of cells and microscopy was performed essentially as described previously.[15,61] LSM 510 Meta NLO Confocal Microscope from Carl Zeiss was used for colocalization studies. Imaging was performed using 63× oil immersion objective lens (NA 1.4). Two, 0.33 μm, middle optical Z-sections were projected and colocalization was analyzed by using LSM 510 (version 3.2) software. Pearson's correlation coefficients for colocalization were calculated by LSM 510 software. Zeiss Axioplan 2 microscope was also used for observing immunofluorescence. Images were captured using the Axiocam (Zeiss) CCD camera and processed with Axiovision 4 software. The number of vesicles (> 0.5 μm and > 0.8 μm) in wild-type and M98K mutant of OPTN-expressing cells were counted in at least 100 cells using Imaris software. Images were further processed using Adobe Photoshop software.

Transferrin uptake. After 24 h of transfection, RGC-5 cells grown on coverslips were washed three times with PBS and incubated with serum-free DMEM for 2 h. Cells were then incubated with 10 μg/ml of Alexa-546 conjugated transferrin in serum-free medium for 1 h at 4°C. Cells were then shifted to 37°C for 15 min for uptake of labeled transferrin. Cells were washed with PBS twice and fixed in 3.7% formaldehyde. For quantitative analysis, the fluorescence intensity of internalized transferrin was measured using ImageJ software (n = 150 cells each for M98K and wild-type OPTN). Normalization of fluorescence intensities of transfected cells was done against nonexpressing cells.

Measuring autophagic flux. For measuring autophagic flux using mCherry-GFP-LC3B or number of autophagosomes formed by GFP-LC3B under various conditions, images were taken using LSM 510 Meta NLO Confocal Microscope from Carl Zeiss with 63× oil immersion objective lens (NA 1.4). Optical Z-sections of 0.4 μm were taken from top to the bottom of the cell (at least 20 to 25 Z-sections). These images were then analyzed using Imaris software (Bitplane, Switzerland) for measuring total number of green dots (or yellow dots) and total number of red dots. Green/yellow dots represent autophagosomes. Only red dots represent autolysosomes, which were calculated by subtracting total red dots with green/yellow dots.

Coimmunoprecipitation and western blotting. For coimmunoprecipitation, RGC-5 cells in 35-mm dishes were either transfected with required plasmids or infected with required adenoviruses. After 24 h, cells were washed with ice-cold PBS and then lysed at 4°C for 20 min in lysis buffer containing 25 mM TRIS-HCl, pH 7.4, 150 mM NaCl, 1.0% Triton X-100, 1 mM PMSF, 0.1% BSA, 5 mM EDTA and protease inhibitor cocktail (Roche Biochemicals, 11697498001). Lysates were centrifuged at 10,000 g for 10 min at 4°C and the supernatant fraction was used for immunoprecipitation using the required antibody or normal IgG as a control antibody. Supernatants were incubated overnight with antibodies. Then, 25 μl protein A/G plus agarose beads (Santa Cruz, sc-2003) were added to the cell lysates for another 2 h at 4°C. The beads containing immune complexes were given three washes in wash buffer (20 mM HEPES pH 7.4, 0.1% Triton X-100, 150 mM NaCl, 10% glycerol, 1 mM PMSF, and protease inhibitors), and then boiled in sample buffer for SDS-PAGE. The samples were resolved on SDS-PAGE and transferred to a nitrocellulose membrane for western blot analysis. Western blotting was performed using standard protocols as described earlier.[61]

Cell death assays. Quantitative analysis of apoptotic cells was performed as described previously.[28] Cells showing loss of refractility, cytoplasmic shrinkage and condensed chromatin were scored as dead cells.

Yeast two-hybrid interaction assays. The procedure followed has been described.[61] Briefly, the yeast strain was transformed with required plasmids. The growth of the colonies on adenine-deficient (Ade^-) plates and color development on $X\text{-}Gal^+$ plates indicated interaction between two proteins.

Statistical analysis. Bar diagrams represent mean ± s.d values. Differences between means were tested using Student's t-test.

Disclosure of Potential Conflicts of Interest

No potential conflicts of interest were disclosed.

Acknowledgments

We thank Dr. Terje Johansen for providing reagents. This work was supported by a grant to G.S. from the Department of Biotechnology, Government of India. G.S. gratefully acknowledges the Department of Science and Technology, Government of India for J C Bose National Fellowship. K.S. is a recipient of a Research Fellowship from the CSIR, New Delhi, India.

Supplemental Materials

Supplemental materials may be found here:
www.landesbioscience.com/journals/autophagy/article/23458

References

1. Rezaie T, Child A, Hitchings R, Brice G, Miller L, Coca-Prados M, et al. Adult-onset primary open-angle glaucoma caused by mutations in optineurin. Science 2002; 295:1077-9; PMID:11834836; http://dx.doi.org/10.1126/science.1066901
2. Maruyama H, Morino H, Ito H, Izumi Y, Kato H, Watanabe Y, et al. Mutations of optineurin in amyotrophic lateral sclerosis. Nature 2010; 465:223-6; PMID:20428114; http://dx.doi.org/10.1038/nature08971
3. Liu Y, Allingham RR. Molecular genetics in glaucoma. Exp Eye Res 2011; 93:331-9; PMID:21871452; http://dx.doi.org/10.1016/j.exer.2011.08.007
4. Ayala-Lugo RM, Pawar H, Reed DM, Lichter PR, Moroi SE, Page M, et al. Variation in optineurin (OPTN) allele frequencies between and within populations. Mol Vis 2007; 13:151-63; PMID:17293779
5. Leung YF, Fan BJ, Lam DS, Lee WS, Tam PO, Chua JK, et al. Different optineurin mutation pattern in primary open-angle glaucoma. Invest Ophthalmol Vis Sci 2003; 44:3880-4; PMID:12939304; http://dx.doi.org/10.1167/iovs.02-0693
6. Kumar A, Basavaraj MG, Gupta SK, Qamar I, Ali AM, Bajaj V, et al. Role of CYP1B1, MYOC, OPTN, and OPTC genes in adult-onset primary open-angle glaucoma: predominance of CYP1B1 mutations in Indian patients. Mol Vis 2007; 13:667-76; PMID:17563717
7. Liu Y, Akafo S, Santiago-Turla C, Cohen CS, Larocque-Abramson KR, Qin X, et al. Optineurin coding variants in Ghanaian patients with primary open-angle glaucoma. Mol Vis 2008; 14:2367-72; PMID:19096531

8. Fuse N, Takahashi K, Akiyama H, Nakazawa T, Seimiya M, Kuwahara S, et al. Molecular genetic analysis of optineurin gene for primary open-angle and normal tension glaucoma in the Japanese population. J Glaucoma 2004; 13:299-303; PMID:15226658; http://dx.doi.org/10.1097/00061198-200408000-00007
9. Alward WL, Kwon YH, Kawase K, Craig JE, Hayreh SS, Johnson AT, et al. Evaluation of optineurin sequence variations in 1,048 patients with open-angle glaucoma. Am J Ophthalmol 2003; 136:904-10; PMID:14597044; http://dx.doi.org/10.1016/S0002-9394(03)00577-4
10. Sripriya S, Nirmaladevi J, George R, Hemamalini A, Baskaran M, Prema R, et al. OPTN gene: profile of patients with glaucoma from India. Mol Vis 2006; 12:816-20; PMID:16885925
11. Hattula K, Peränen J. FIP-2, a coiled-coil protein, links Huntingtin to Rab8 and modulates cellular morphogenesis. Curr Biol 2000; 10:1603-6; PMID:11137014; http://dx.doi.org/10.1016/S0960-9822(00)00864-2
12. Chalasani ML, Swarup G, Balasubramanian D. Optineurin and its mutants: molecules associated with some forms of glaucoma. Ophthalmic Res 2009; 42:176-84; PMID:19672125; http://dx.doi.org/10.1159/000232400
13. Zhu G, Wu CJ, Zhao Y, Ashwell JD. Optineurin negatively regulates TNFalpha- induced NF-kappaB activation by competing with NEMO for ubiquitinated RIP. Curr Biol 2007; 17:1438-43; PMID:17702576; http://dx.doi.org/10.1016/j.cub.2007.07.041
14. Wild P, Farhan H, McEwan DG, Wagner S, Rogov VV, Brady NR, et al. Phosphorylation of the autophagy receptor optineurin restricts Salmonella growth. Science 2011; 333:228-33; PMID:21617041; http://dx.doi.org/10.1126/science.1205405
15. Nagabhushana A, Chalasani ML, Jain N, Radha V, Rangaraj N, Balasubramanian D, et al. Regulation of endocytic trafficking of transferrin receptor by optineurin and its impairment by a glaucoma-associated mutant. BMC Cell Biol 2010; 11:4; PMID:20085643; http://dx.doi.org/10.1186/1471-2121-11-4
16. Ying H, Shen X, Park B, Yue BY. Posttranslational modifications, localization, and protein interactions of optineurin, the product of a glaucoma gene. PLoS One 2010; 5:e9168; PMID:20161783; http://dx.doi.org/10.1371/journal.pone.0009168
17. Rezaie T, Sarfarazi M. Molecular cloning, genomic structure, and protein characterization of mouse optineurin. Genomics 2005; 85:131-8; PMID:15607428; http://dx.doi.org/10.1016/j.ygeno.2004.10.011
18. Nagabhushana A, Bansal M, Swarup G. Optineurin is required for CYLD-dependent inhibition of TNFα-induced NF-κB activation. PLoS One 2011; 6:e17477; PMID:21408173; http://dx.doi.org/10.1371/journal.pone.0017477
19. Sahlender DA, Roberts RC, Arden SD, Spudich G, Taylor MJ, Luzio JP, et al. Optineurin links myosin VI to the Golgi complex and is involved in Golgi organization and exocytosis. J Cell Biol 2005; 169:285-95; PMID:15837803; http://dx.doi.org/10.1083/jcb.200501162
20. Sudhakar C, Nagabhushana A, Jain N, Swarup G. NF-kappaB mediates tumor necrosis factor alpha-induced expression of optineurin, a negative regulator of NF-kappaB. PLoS One 2009; 4:e5114; PMID:19340308; http://dx.doi.org/10.1371/journal.pone.0005114
21. Kachaner D, Filipe J, Laplantine E, Bauch A, Bennett KL, Superti-Furga G, et al. Plk1-dependent phosphorylation of optineurin provides a negative feedback mechanism for mitotic progression. Mol Cell 2012; 45:553-66; PMID:22365832; http://dx.doi.org/10.1016/j.molcel.2011.12.030
22. Ying H, Yue BY. Cellular and molecular biology of optineurin. Int Rev Cell Mol Biol 2012; 294:223-58; PMID:22364875; http://dx.doi.org/10.1016/B978-0-12-394305-7.00005-7
23. Journo C, Filipe J, About F, Chevalier SA, Afonso PV, Brady JN, et al. NRP/Optineurin Cooperates with TAX1BP1 to potentiate the activation of NF-kappaB by human T-lymphotropic virus type 1 tax protein. PLoS Pathog 2009; 5:e1000521; PMID:19609363; http://dx.doi.org/10.1371/journal.ppat.1000521
24. Mankouri J, Fragkoudis R, Richards KH, Wetherill LF, Harris M, Kohl A, et al. Optineurin negatively regulates the induction of IFNbeta in response to RNA virus infection. PLoS Pathog 2010; 6:e1000778; PMID:20174559; http://dx.doi.org/10.1371/journal.ppat.1000778
25. Gleason CE, Ordureau A, Gourlay R, Arthur JS, Cohen P. Polyubiquitin binding to optineurin is required for optimal activation of TANK-binding kinase 1 and production of interferon β. J Biol Chem 2011; 286:35663-74; PMID:21862579; http://dx.doi.org/10.1074/jbc.M111.267567
26. Schwamborn K, Weil R, Courtois G, Whiteside ST, Israël A. Phorbol esters and cytokines regulate the expression of the NEMO-related protein, a molecule involved in a NF-kappa B-independent pathway. J Biol Chem 2000; 275:22780-9; PMID:10807909; http://dx.doi.org/10.1074/jbc.M001500200
27. Bond LM, Peden AA, Kendrick-Jones J, Sellers JR, Buss F. Myosin VI and its binding partner optineurin are involved in secretory vesicle fusion at the plasma membrane. Mol Biol Cell 2011; 22:54-65; PMID:21148290; http://dx.doi.org/10.1091/mbc.E10-06-0553
28. Chalasani ML, Radha V, Gupta V, Agarwal N, Balasubramanian D, Swarup G. A glaucoma-associated mutant of optineurin selectively induces death of retinal ganglion cells which is inhibited by antioxidants. Invest Ophthalmol Vis Sci 2007; 48:1607-14; PMID:17389490; http://dx.doi.org/10.1167/iovs.06-0834
29. Park B, Ying H, Shen X, Park JS, Qiu Y, Shyam R, et al. Impairment of protein trafficking upon overexpression and mutation of optineurin. PLoS One 2010; 5:e11547; PMID:20634958; http://dx.doi.org/10.1371/journal.pone.0011547
30. Chi ZL, Akahori M, Obazawa M, Minami M, Noda T, Nakaya N, et al. Overexpression of optineurin E50K disrupts Rab8 interaction and leads to a progressive retinal degeneration in mice. Hum Mol Genet 2010; 19:2606-15; PMID:20388642; http://dx.doi.org/10.1093/hmg/ddq146
31. Shen X, Ying H, Qiu Y, Park JS, Shyam R, Chi ZL, et al. Processing of optineurin in neuronal cells. J Biol Chem 2011; 286:3618-29; PMID:21059646; http://dx.doi.org/10.1074/jbc.M110.175810
32. Vaibhava V, Nagabhushana A, Chalasani ML, Sudhakar C, Kumari A, Swarup G. Optineurin mediates a negative regulation of Rab8 by the GTPase-activating protein TBC1D17. J Cell Sci 2012; 125:5026-39; PMID:22854040; http://dx.doi.org/10.1242/jcs.102327
33. Son JH, Shim JH, Kim KH, Ha JY, Han JY. Neuronal autophagy and neurodegenerative diseases. Exp Mol Med 2012; 44:89-98; PMID:22257884; http://dx.doi.org/10.3858/emm.2012.44.2.031
34. Maxfield FR, McGraw TE. Endocytic recycling. Nat Rev Mol Cell Biol 2004; 5:121-32; PMID:15040445; http://dx.doi.org/10.1038/nrm1315
35. Matsui T, Itoh T, Fukuda M. Small GTPase Rab12 regulates constitutive degradation of transferrin receptor. Traffic 2011; 12:1432-43; PMID:21718402; http://dx.doi.org/10.1111/j.1600-0854.2011.01240.x
36. Tachiyama R, Ishikawa D, Matsumoto M, Nakayama KI, Yoshimori T, Yokota S, et al. Proteome of ubiquitin/MVB pathway: possible involvement of iron-induced ubiquitylation of transferrin receptor in lysosomal degradation. Genes Cells 2011; 16:448-66; PMID:21392187; http://dx.doi.org/10.1111/j.1365-2443.2011.01499.x
37. Matsui T, Fukuda M. Small GTPase Rab12 regulates transferrin receptor degradation: Implications for a novel membrane trafficking pathway from recycling endosomes to lysosomes. Cell Logist 2011; 1:155-8; PMID:22279614; http://dx.doi.org/10.4161/cl.1.4.18152
38. Krishnamoorthy RR, Agarwal P, Prasanna G, Vopat K, Lambert W, Sheedlo HJ, et al. Characterization of a transformed rat retinal ganglion cell line. Brain Res Mol Brain Res 2001; 86:1-12; PMID:11165366; http://dx.doi.org/10.1016/S0169-328X(00)00224-2
39. Van Bergen NJ, Wood JP, Chidlow G, Trounce IA, Casson RJ, Ju WK, et al. Recharacterization of the RGC-5 retinal ganglion cell line. Invest Ophthalmol Vis Sci 2009; 50:4267-72; PMID:19443730; http://dx.doi.org/10.1167/iovs.09-3484
40. Fujita H, Sasano E, Yasunaga K, Furuta K, Yokota S, Wada I, et al. Evidence for distinct membrane traffic pathways to melanosomes and lysosomes in melanocytes. J Investig Dermatol Symp Proc 2001; 6:19-24; PMID:11764280; http://dx.doi.org/10.1046/j.0022-202x.2001.00009.x
41. Mizushima N, Komatsu M. Autophagy: renovation of cells and tissues. Cell 2011; 147:728-41; PMID:22078875; http://dx.doi.org/10.1016/j.cell.2011.10.026
42. Sridhar S, Botbol Y, Macian F, Cuervo AM. Autophagy and disease: always two sides to a problem. J Pathol 2012; 226:255-73; PMID:21990109; http://dx.doi.org/10.1002/path.3025
43. Pankiv S, Clausen TH, Lamark T, Brech A, Bruun JA, Outzen H, et al. p62/SQSTM1 binds directly to Atg8/LC3 to facilitate degradation of ubiquitinated protein aggregates by autophagy. J Biol Chem 2007; 282:24131-45; PMID:17580304; http://dx.doi.org/10.1074/jbc.M702824200
44. Kabeya Y, Mizushima N, Ueno T, Yamamoto A, Kirisako T, Noda T, et al. LC3, a mammalian homologue of yeast Apg8p, is localized in autophagosome membranes after processing. EMBO J 2000; 19:5720-8; PMID:11060023; http://dx.doi.org/10.1093/emboj/19.21.5720
45. Mizushima N, Yamamoto A, Hatano M, Kobayashi Y, Kabeya Y, Suzuki K, et al. Dissection of autophagosome formation using Apg5-deficient mouse embryonic stem cells. J Cell Biol 2001; 152:657-68; PMID:11266458; http://dx.doi.org/10.1083/jcb.152.4.657
46. Levy JE, Jin O, Fujiwara Y, Kuo F, Andrews NC. Transferrin receptor is necessary for development of erythrocytes and the nervous system. Nat Genet 1999; 21:396-9; PMID:10192390; http://dx.doi.org/10.1038/7727
47. Rouault TA, Cooperman S. Brain iron metabolism. Semin Pediatr Neurol 2006; 13:142-8; PMID:17101452; http://dx.doi.org/10.1016/j.spen.2006.08.002
48. LaVaute T, Smith S, Cooperman S, Iwai K, Land W, Meyron-Holtz E, et al. Targeted deletion of the gene encoding iron regulatory protein-2 causes misregulation of iron metabolism and neurodegenerative disease in mice. Nat Genet 2001; 27:209-14; PMID:11175792; http://dx.doi.org/10.1038/84859
49. Lamark T, Kirkin V, Dikic I, Johansen T. NBR1 and p62 as cargo receptors for selective autophagy of ubiquitinated targets. Cell Cycle 2009; 8:1986-90; PMID:19502794; http://dx.doi.org/10.4161/cc.8.13.8892
50. Weidberg H, Shvets E, Elazar Z. Biogenesis and cargo selectivity of autophagosomes. Annu Rev Biochem 2011; 80:125-56; PMID:21548784; http://dx.doi.org/10.1146/annurev-biochem-052709-094552
51. Wong E, Cuervo AM. Autophagy gone awry in neurodegenerative diseases. Nat Neurosci 2010; 13:805-11; PMID:20581817; http://dx.doi.org/10.1038/nn.2575
52. Liou W, Geuze HJ, Geelen MJ, Slot JW. The autophagic and endocytic pathways converge at the nascent autophagic vacuoles. J Cell Biol 1997; 136:61-70; PMID:9008703; http://dx.doi.org/10.1083/jcb.136.1.61

53. Tooze J, Hollinshead M, Ludwig T, Howell K, Hoflack B, Kern H. In exocrine pancreas, the basolateral endocytic pathway converges with the autophagic pathway immediately after the early endosome. J Cell Biol 1990; 111:329-45; PMID:2166050; http://dx.doi.org/10.1083/jcb.111.2.329
54. Longatti A, Lamb CA, Razi M, Yoshimura S, Barr FA, Tooze SA. TBC1D14 regulates autophagosome formation via Rab11- and ULK1-positive recycling endosomes. J Cell Biol 2012; 197:659-75; PMID:22613832; http://dx.doi.org/10.1083/jcb.201111079
55. Chen Y, Klionsky DJ. The regulation of autophagy - unanswered questions. J Cell Sci 2011; 124:161-70; PMID:21187343; http://dx.doi.org/10.1242/jcs.064576
56. Eisenberg-Lerner A, Bialik S, Simon HU, Kimchi A. Life and death partners: apoptosis, autophagy and the cross-talk between them. Cell Death Differ 2009; 16:966-75; PMID:19325568; http://dx.doi.org/10.1038/cdd.2009.33
57. Shivakrupa R, Radha V, Sudhakar Ch, Swarup G. Physical and functional interaction between Hck tyrosine kinase and guanine nucleotide exchange factor C3G results in apoptosis, which is independent of C3G catalytic domain. J Biol Chem 2003; 278:52188-94; PMID:14551197; http://dx.doi.org/10.1074/jbc.M310656200
58. Sadasivam S, Gupta S, Radha V, Batta K, Kundu TK, Swarup G. Caspase-1 activator Ipaf is a p53-inducible gene involved in apoptosis. Oncogene 2005; 24:627-36; PMID:15580302; http://dx.doi.org/10.1038/sj.onc.1208201
59. Swarup G. How to design a highly effective siRNA. J Biosci 2004; 29:129-31; PMID:15295207; http://dx.doi.org/10.1007/BF02703408
60. Yu JY, DeRuiter SL, Turner DL. RNA interference by expression of short-interfering RNAs and hairpin RNAs in mammalian cells. Proc Natl Acad Sci U S A 2002; 99:6047-52; PMID:11972060; http://dx.doi.org/10.1073/pnas.092143499
61. Gupta V, Swarup G. Evidence for a role of transmembrane protein p25 in localization of protein tyrosine phosphatase TC48 to the ER. J Cell Sci 2006; 119:1703-14; PMID:16595549; http://dx.doi.org/10.1242/jcs.02885